Development of a Highly Flexible and Stretchable Tubular Shape Tactile Sensor Array

A THESIS

SUBMITTED TO THE FACULTY OF THE GRADUATE SCHOOL

OF THE UNIVERSITY OF MINNESOTA

BY

YUHANG SUN

IN PARTIAL FULFILLMENT OF THE REQUIREMENTS

FOR THE DEGREE OF

MASTER OF SCIENCE

Advisers: Dr. Jing Bai and Dr. Debao Zhou

August 2016

Acknowledgements

I would like to thank my advisor, Prof. Jing Bai. For all the help she has given me on both research and life. She genuinely cares about all her students and patiently inspires them to trust and improve themselves.

I also want to thank my co-advisor Prof. Debao Zhou. He provided me all the essential support for the research work and enlightened me the way to explore the possibility for improvement on both the project and myself.

And thanks also goes to Prof. Burns, I really enjoyed your lectures and beef jerkies. It's very nice of you to take your time off your busy schedule for my defense.

My gratitude goes to my friend Dr. Haopeng Wang as well. His research on the first stage was a wonderful reference for me to go forward. And my friend Eliah Hauser, his closely associate on the whole summer is a vital boost on the project.

In addtion, I would like to express my appreciation to all the staff in Minnesota Nano Center, without your patient guide, I can hardly carry out these good data.

Finally, I sinerely acknowledge the graduate research assistantship support from the Grant-in-Aid fund under Dr. Zhou and the MnDrive fund under Drs. Zhou and Bai.

Thank all the fellow graduate students, faculty and staff, who make our department and this campus a warm family.

Dedication

To my wife Rang and my little daughter Olivia, who always understand and warm my heart.

To City of Duluth, a sweet dream by Lake Superior.

Yuhang Sun

June 2016

Abstract

Highly flexible skin-like sensors, such as electrical skin (e-skin) sensor for pressure measurement, have the potential to provide quantitative physical contact assessments, when equipped on household and medical devices to benefit human society. One of the promising applications is to monitor the contact pressure of a colonoscope to the colonic wall during a colonoscopy to reduce the possibility of perforation and hemorrhaging .Colon, as the largest intestine, is a long winding tube at the end of human's digestive tract. Many disorders affect the colon's ability to work properly, thus the American Cancer Society suggests that citizens over 50 years old should be subject to a colon screen test. However, risks do exist during colonoscopy. A rate of 0.19% perforation occurs in the diagnostic colonoscopy. Many attempts have been made to fabricate highly stretchable electronic devices, but no effort has been made to design or investigate the mechanical behaviors of a tubular-shaped e-skin that meet the need for controlling the risks during colonoscopy. In this project, a high performance three-layer tactile sensor array was designed and fabricated, and a pressure detection system was set up as well. The operating mode was thoroughly investigated and the pressure detection on curved surface, such as a tube was realized. A detailed study about false positive error was performed to improve the sensor’s reliability and accuracy. Based on a tubular-shaped, highly flexible skin-like sensor array we developed, we conducted both modeling and experimental studies on the change of the maximum pressure distribution of a tubular e-skin sensor under various bending conditions with and without external compressive forces. These studies revealed the value of the maximum stress on a tubular shaped e-skin sensor array when bent. The measuring errors due to bending in pressure detection during colonoscopy can be quantified for compensation. Thus, high accuracy diagnose can be achieved. Based on all these work, the pressure detection in the colon-simulator was successfully realized. The results could also be used to address strategies on optimizing the design of tactile sensors for other medical applications

Table of Contents

Acknowledgements ..... **I**

Dedication ..... **II**

Abstract ..... **III**

List of Figures ..... **VI**

List of Tables ..... **VIII**

CHAPTER 1 Introduction **1**

1.1 Research Objective **1**

1.2 Overview of Flexible Electronic Device **5**

1.3 Goal and Contents of Current Research Work **15**

1.4 Structure of Dissertation **17**

CHAPTER 2 Design of Tactile Sensor System **18**

2.1 Structure of Tactile Sensor **18**

2.2 Components of Sensor Arrays **20**

2.2.1 PDMS **20**

2.2.2 Dragon Skin **22**

2.2.3 Silver Nanowire **23**

2.2.4 Pressure Sensitive Electric Conductive Elastomer **25**

2.3 Fabrication and Test of Stretchable Electrode **27**

2.3.1 Fabrication of Flexible Electrode by Spin Coating **28**

2.3.2 Fabrication of Flexible Electrode by Controlled Spacing Extrusion **30**

2.3.3 Resistance Measurement after Metalization and Stretchability Comparison **32**

2.3.4 Fatigue Test **34**

2.4 The Design of Scanning Circuit **37**

2.5 Main Components of Data Acquisition System **38**

CHAPTER 3 Performance Testing of Sensor System the Under Bending Deformation and Applied Force 42

3.1 The Pressure-Resistance Characterization of Sensor Cell 42

3.2 Internal Pressure Investigation 44

3.3 Mathematical Modeling and Simulation 46

3.4 Sensor Test with Applied Force 51

CHAPTER 4 Pressure Detection in Colon-Simulator 54

4.1 Colon Simulator 54

4.2 Insertion Test and Real Time Pressure Detection 55

CHAPTER 5 Conclusion and Future Recommendations 59

References 63

Appendix: Publication from This Work 68

List of Figures

Fig. 1.1	ASIMO learns to climb a vertical ladder with tactile sensors embedded	P2
Fig. 1.2	Robot PR2 touches an experiment participant	P3
Fig. 1.3	Schematic for colonoscopy	P4
Fig. 1.4	Iimage of flexible sensor array based on organic transistors by Someya's group	P6
Fig. 1.5	Illustration of wavy buckled structure proposed by Rogers' group	P7
Fig. 1.6	A schematic of a cross-section SWNT PMOS inverter on a flexible polyimide substrate and photograph of a collection of SWNT transistors	P9
Fig. 1.7	(a) Schematic of passive and active layers of the e-skin done by Javey's group; (b) Structure of pressure visualized sensor	P9
Fig. 1.8	(a) Flexible sensor array based on active-matrix circuitry; (b)Self-healing composite mixed by oligomer chains and μNi particles	P10
Fig. 1.9	(a) Flexibility achieved of traditional materials by wavy structure; (b) Finger-shaped flexible tactile sensor made by Si and Au based materials	P11
Fig. 1.10	Biodegradable graphene nanosensor	P12
Fig. 1.11	(a)-(e) CNT-PDMS based interlock structure e-skin by Ko's goup	P13
Fig. 1.12	Capacitive sensor mode made by gold thin film/PDMS by Cotton et al.	P14
Fig. 1.13	T.Someya's group designed an Ag electrode coated transistor interconnected by elastic conductors on PDMS sheet which can sustain some biaxial stretching	P15
Fig. 2.1	Diagram of sensor layers	P19
Fig. 2.2	PDMS silicone(Sylgard 184 silicone elastomer base) from Dow Corning®	P20
Fig. 2.3	Dragon Skin® Platinum Cure kit 10 medium	P22
Fig. 2.4	SEM Picture of SLV-NW-90 AgNW from blue nano®	P23
Fig. 2.5	SLV-NW-90 AgNW pack from Blue Nano®	P24
Fig. 2.6	Conductive elastomer CS57-7RSC	P25
Fig. 2.7	Fabrication procedure of stretchable electrodes	P28
Fig. 2.8	Fabrication of electrode layer by extrusion	P30
Fig. 2.9	Electrodes test after metalization	P33
Fig. 2.10	Fatigue test setup and resistance measure under different Strain rates using a tensile testing stage after fatigure	P34

	test	
Fig. 2.11	Resistance of an AgNW/Dragon Skin stretchable conductive strip as a function of tensile strain at different stretching cycles	P35
Fig. 2.12	Schematic of tactile array system	P37
Fig. 2.13	Phidget InterfaceKit 8/8/8 Data Acquisition Cards	P39
Fig. 2.14	The SU-8 2075 mold	P40
Fig. 2.15	Exploded view of the assembled e-skin sensor	P41
Fig. 3.1	Property of the piezo-resistive rubber provided by manufacuture(PCR Japan)	P42
Fig. 3.2	Experimental set-up for piezoresistive characterization of the sensor cells	P43
Fig. 3.3	Piezo-resistive response of sensor with pressure	P44
Fig. 3.4	Bending test of the tactile-sensor system(without applied pressure)	P45
Fig. 3.5	Experimental results: bending curvature vs internal pressure	P46
Fig. 3.6	Simulation results: bending curvature vs internal pressure	P50
Fig. 3.7	Comparison between experimental and simulation results	P51
Fig. 3.8	Recalibrate the robot and conduct experiment taken with constant external pressure applied by Epson Scara G3 robot	P52
Fig. 3.9	Comparison of corrected experimental data with simulation data when bent against 200mm radii pipe	P53
Fig. 4.1	Colonoscope training mode by Kyoto Kagaka.Co	P54
Fig. 4.2	Two sensor patches integrated on the tube	P55
Fig. 4.3	Real time pressure detection in colon-simulator when apply pressure on sensor	P56
Fig. 4.4	Relationship between brightness value and applied pressure with bending curvature of 500mm	P57
Fig. 5.1	Illustration of the 3-D injection process by 3D-printer and suitable nozzle tip	P60

List of Tables

Table 1-1	Basic criteria for tactile sensor system	P8
Table 2-1	Major properties of PDMS elastomer	P21
Table 2-2	Physical property of CS57-7RSC	P26
Table 2-3	Parameters for spin coating in step#1 and #4	P27
Table 2-4	Parameters for different PVD processes	P31
Table 2-5	Resistances of the stretchable electrodes after different metallization rountines	P32
Table 2-6	Stamp specification of BS2p40	P38

CHAPTER 1

Introduction

In this chapter, we will illustrate the motivation of current research, provide a thorough overview of flexible sensor technology and introduce the contents of our work as well as the outline of this thesis.

1.1 Research Objective

Colonoscopy is a common endoscopic examination to provide visual diagnosis for colorectal cancer lesions in human colon. People older than 50-years old are suggested to take a colonoscopy every ten years [1]. However, risks do exist during the diagnostic colonoscopy, a rate of 0.1% perforation does occur during colonoscopy, which are fatal threats to patients [2]. In fact, quite small pressure could already lead to diverticular hemorrhage on a colon wall, while even experienced doctors are unlikely to avoid the unwanted pressure inside the colon during the whole procedure. In this case, a high sensitivity and stretchability tactile pressure measurement sensor will be a practical and crucial supplement to reduce the risks, and meliorate the patients' experience of colonoscopy. It could be a useful training tool for new therapists as well.

Artificial electronic skin-like devices, which is also known as 'e-skin', is the best candidate that has potential to meet all the needs for this. As we all know, skin is the largest sensory organ in Human body. There are many types of sense receptors on it. As one of the sensing function of human skin, information generated by physical contact will be transformed into electrical signals and be sent the brain, the central nervous system. Motivated by the possibility to build this kind of multi-sensory

surface, considerable research efforts have been put to create flexible electronic devices like human-skin, which is the e-skin. The efforts to create e-skins are mainly led by two aspects: one is make the e-skin applicable to autonomous artificial intelligence; and the other is to be applicable in or on human bodies to provide an unprecedented level of diagnostic and monitoring capabilities [3]. It is assumed that the proposed e-skin sensor array devices has the ability to bend, stretch, compress, fold or twist for various of potential biological applications[4]. These characteristics are supposed to be achieved by two main strategies: (1) designing new structural constructs using conventional materials or (2) assembling a device from new type stretchable materials [5, 6]. Inspired by their foreseeable capability to revolutionize the humanoid health care products, i.e. robots and the health monitoring equipment, researchers have come up with various of strategies to improve the tactile sensors' performance in many ways.

As the primary function of skin, mechanical force detection gives us the sense of touch with our surroundings, thus the key ability of flexible electronic devices(e-skins) is to measure the physical contact between sensor and environment [7]. Many of studies have shown that flexible tactile sensors can be integrated on medical instruments to work as haptic perception components [8-11]. They are adapted to aid the instrument or robot to manipulate objects while simultaneously sensing and reasoning their environments. Firstly they provide the information about the forces and positions of the contact, then these information can be fed back to the robots, optimize the handling operations [12, 13].

To mimic the properties of human skin successfully, three sub-tasks are generally needed to be fulfilled. One is to provide e-skin with appropriate range of tactile sensitivity. The second is the ability to distinguish a variety of mechanical

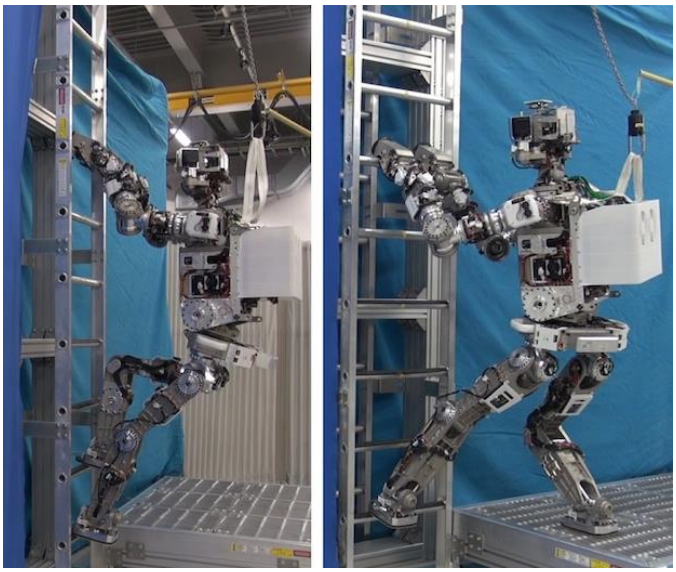

Fig. 1.1 ASIMO learns to climb a vertical ladder with tactile sensors embedded

stimuli such as normal pressure, lateral strain, and bending, in order to allow object manipulation, grasp control, and texture determination. The last is that, the e-skin has to be stretchable such that it can be conformable on arbitrarily curved and moving surfaces, such as joints, and can withstand repeated and prolonged mechanical stress, such as bending and twisting [14].

The innovation of flexible tactile sensors is favored by both industrial and household applications, especially for some extreme conditions due to its pivotal advantages. After the Fukushima crisis in Japan, Honda speed up the improvement of its humanoid robot ASIMO in order to provide help in some dangerous situations in nuclear pollution areas [15]. ASIMO, which is designated to work in offices for heavy labor mitigation, did have the limitation to crawl on curved surface or get real time

response from the surrounding due to lack of precise tactile sensor. With more advanced sensor embedded, ASIMO will be able to adjust subsequent contact positions to compensate for some errors and realize a bidirectional motion.

In aspect of household intelligent devices, optimized tactile measurement is a cornerstone for any autonomous progress. Charles's group in Georgia Tech developed the PR2 robot to fulfill the potential for robots to assist the daily living of older adults and provide nursing aid in health care tasks [16]. Since the robot should initiate the

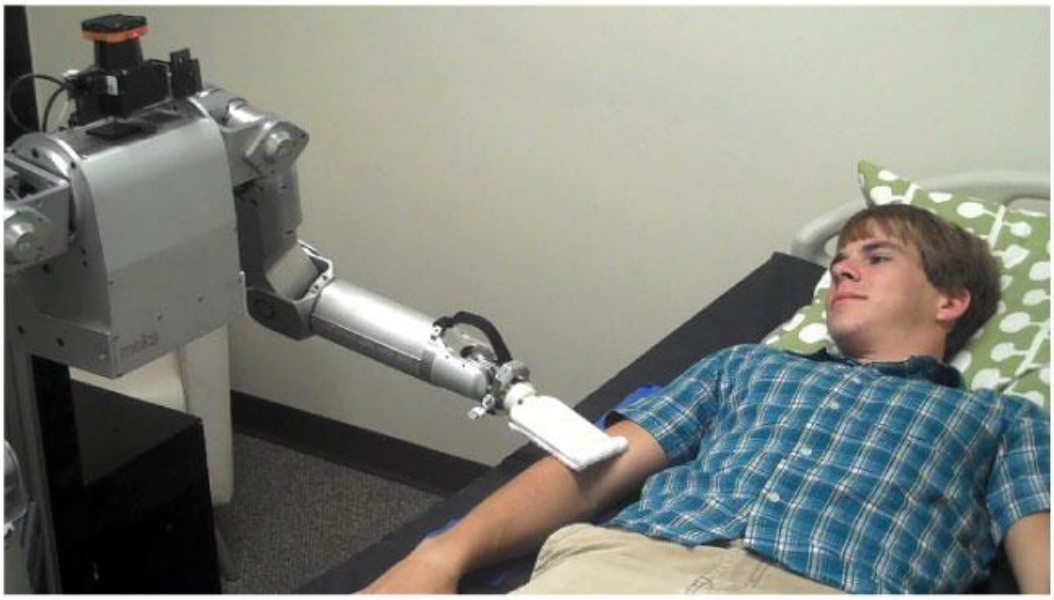

Fig. 1.2 Robot PR2 touches an experiment participant

physical contact with human's body, tactile measurement sensors become one of the most crucial components for the device, Charles et al. embedded compliant enough sensors on the robot's arm to get haptic sensing in order to deal with varieties of real time applications [17].

Back to the goal of our research, a colonoscope is a long, thin and flexible tube whose length can range from 1.25m to 1.80m. It will be inserted from bottom of patient and run through the colon. Thus unpredictable situation may happen anytime,

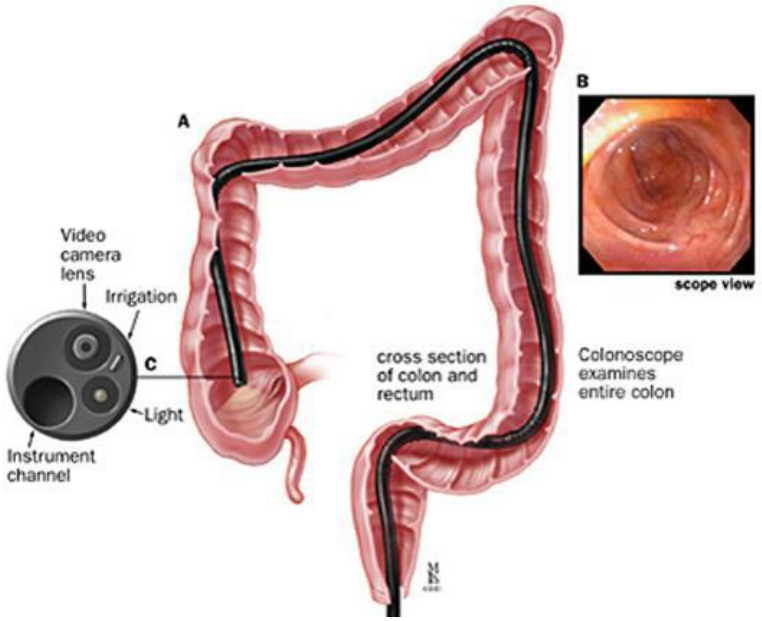

Fig. 1.3 Schematic for colonoscopy

any spot during the test. This brings higher requirements for tactile sensor design, and a series of new issues will occur in fabricating and testing process. Generally speaking, development of a tubular shape highly flexible and stretchable tactile sensor could be both a more compelling and a more challenging topic.

1.2 Overview of Flexible Electronic Device

The originality of creating stretchable electronic devices was in many ways inspired by science fiction from 1970s, and shortly after that, George Lucas depicted a scene showing a robot installing a full sensory perception hand on the main character, Luke Skywalker, which provided the vision of stretchable electronics devices(e-skin) in nowadays and future [18]. Benefit from the important advancements made in

materials science, development of tactile sensor has got significant progress since the new century began. More new features that mimic human characters have been approached and a few of them have been partly realized [19]. Now the primary focus of e-skin research is to bestow the mechanically property of human skin on the tactile sensors, which can be facilitated by: (1) explore new types of sensitive pressure transformable materials [20]; (2) take advantages of new manufacturing technology [21]; (3) simulate the multifunctional nature of skin [22];(4) generate the data fusion mode for typical sensing mechanism [23].

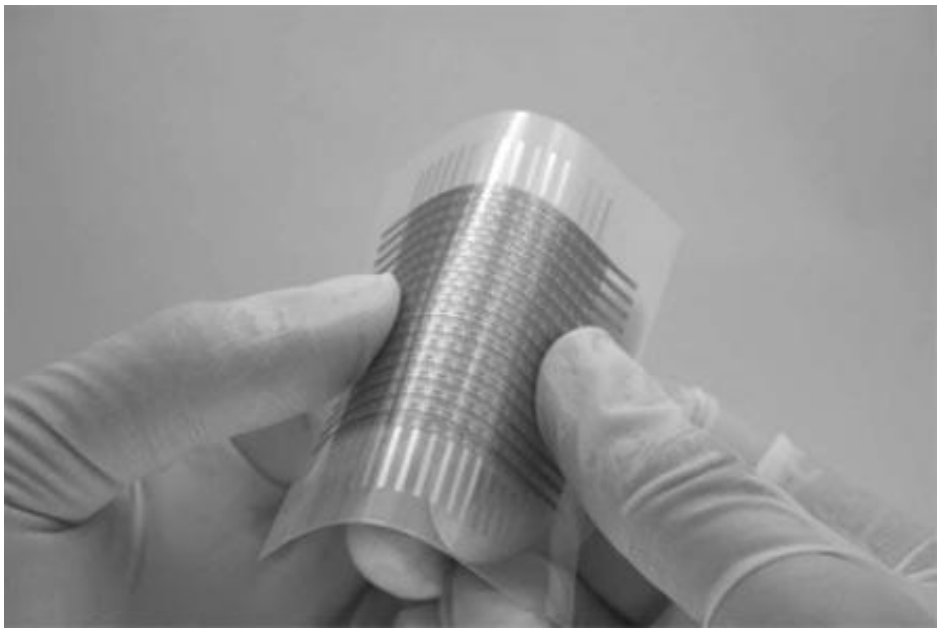

Fig. 1.4 Iimage of flexible sensor array based on organic transistors by Someya's group

In 2004, Someya et al. developed a flexible active matrix matrix, which is used to read out pressure images from the sensors, the whole matrix is bendable because all of the layers with the exception of the electrodes are made of soft materials, this is the first time that good flexibility obtained with relatively large sensor patch area [24].

One year later, Rogers' Group firstly came up with a widely applicable routine of

building stretchable and flexible electronic devices with traditional inorganic materials like metal ribbons. The way is to firstly bond the conducting ribbons on a pre-strain elastomer substrate by vacuum deposition processes, then release the pre-strain to induce compressive force and non-linear buckling. The buckling methods became the most popular strategy for utilizing the traditional materials for e-skin designs. This geometric layout is widely applicable for creating stretchable conductors, transistors, diodes, even fully integrated systems like hemispherical electronic eye cameras. However, the drawback is kind of significant, that is the conducting ribbons can hardly achieve long-term adhesion on the substrate, which reveal reliability issues on these devices.

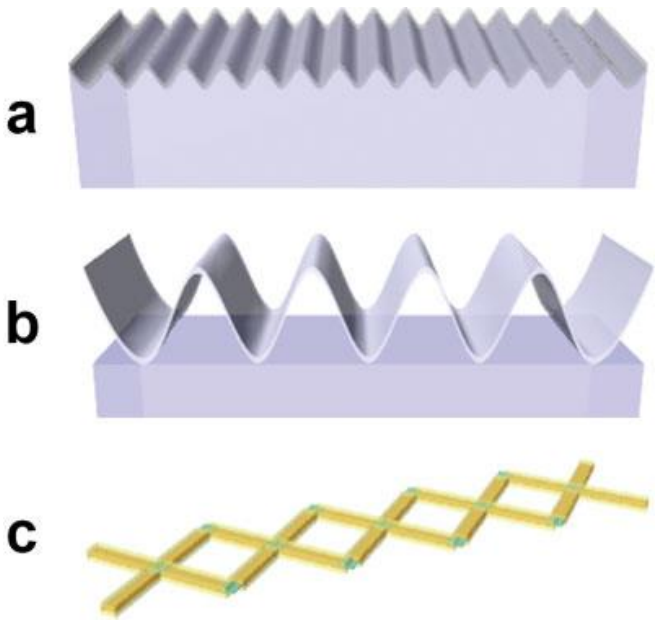

Fig. 1.5 Illustration of wavy buckled structure proposed by Rogers' group

In 2006, Ohmura Y et al utilized several modules that contains pressure-sensitive element to attach on slightly curved surface, and use serial bus to connect each modules in order to measure the pressure distribution. This kind of "cut and paste tactile sensors" provided a possiblity to implement large number of sensing elements

on simple or static 3-D surface, while may not applicable for the dyanmic curved surface. Even though, this principle Ohmura proposed was follwed by lots of research groups and it did provide quotable experience for the latter works about large-area

Table 1-1 basic criteria for tactile sensor system

Conformability	The skin should be applicable to arbitrarily curved surfaces, without specifically fabricating different sensor units for each curved part
Compliance	The sensor should have a soft surface
Installation space	kept to a minimum since inside of the robot or medical devices is full of mechanisms and circuits.
Area coverage	as large as possible
Weight	light-weight since it potentially has to cover the entire body surface which is a large area
Power consumption	The power consumed by the individual tactile elements should be low
Size	The individual sensing elements should be of small size
Toughness	The skin should be tough, and robust against impact and shear forces.
Manufacturability	The skin should be easy to manufacture.
Dynamic range and sensitivity	The sensors should be able to detect contact between light touch and total bodyweight.

tactile sensing. In the article, Ohmura's group concluded ten basic criterias of

accreditable tactile sensor system(e-skins) as follwing:

In 2008, Cao and coworkers fabricated a carbon-based semiconductor composed ofsub-monolayer, random network of single-wall CNT to yield small scale integrated circuits. Those circuits are made up by ~100 transistors on plastic substrates. This propotype provided a attractive routine for the construction of small flexible device[25].

In 2010, Ali Javey and co-workers apply the contact printing method to assemble Ge/Si core/shell NW arrays on a polyimide substrate, and groud the source power supply throungh PSR(pressure sensitive rubber), as long as the PSR get pressure, the conductivity changes, the property of the device will change as well, so they can exam

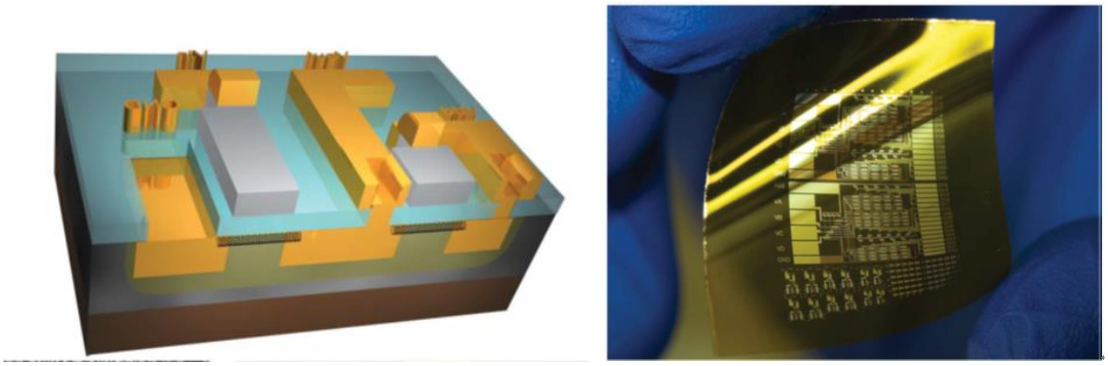

Fig. 1.6 A schematic of a cross-section SWNT PMOS inverter on a flexible polyimide substrate and photograph of a collection of SWNT transistors

the strain induced signal to obtain the pressure on it [26]. The function range of this e-skin can reach up to 2 kpa&5Hz, the response time is within 0.1s. Later in 2013, Ali's group upgraded the flexible sensor, by utilizing the PSR, they integrated OLED with TFT to make a sensor array which can display the contact pressure intensity visually [27].

In 2011, Zhenan Bao and coworkers developed a skin-like stretchable array of sensors based on electrodes composed of spray-coated CNTs sandwiching an ultrasoft

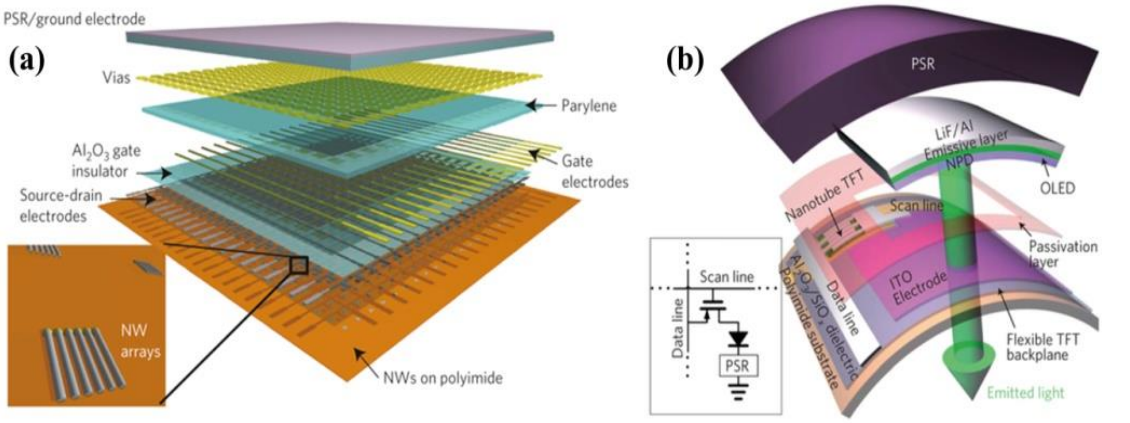

Fig. 1.7 (a) Schematic of passive and active layers of the e-skin done by Javey's group; (b) Structure of pressure visualized sensor

dielectric layer(PDMS), the PDMS layer is nearly transparent with decent elasticity, the overall stretchability can be up to 100%, the embeded crossbar CNTs networks provide passive matrix muliplexing for pressure and strain measurement. The buckled

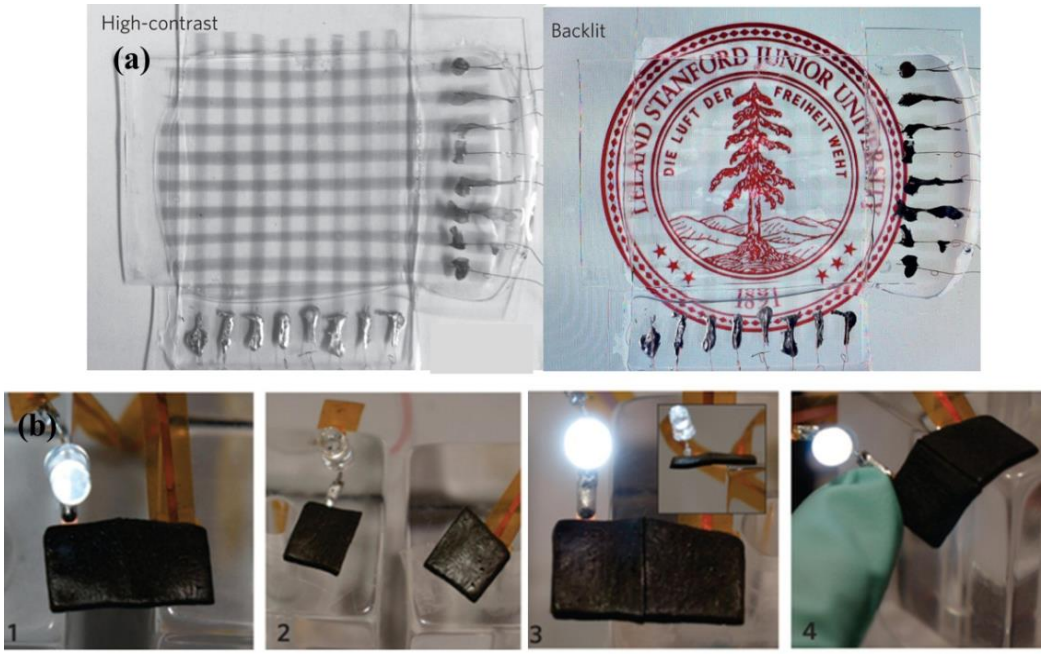

Fig. 1.8 (a) Flexible sensor array based on active-matrix circuitry; (b)Self-healing composite mixed by oligomer chains and μNi particles

CNT and the curly network enhanced the sensor's overall stretchability a lot, while both compression and tension will affect the capacitive signal, thus this sensor array may not be suitable for curved or dyanamic surfaces [28]. A year later, Bao's group reported their photoelectronic pressure sensor array, it is noted that transparency gained increasingly interest in the tactile sensor designs as good transparency will contribute to light absorption of the solar enegry drived components in these devices [29]. Later, they demonstrated the design of self-healing composite by interact oligomer chains with μNi particles, the composite has fair flexibility and the resistance varies inversly with applied flexion and tactile force. the initial conductivity can be restored with 90% efficiency of 15s, and the mechanical properties can be completely restored after 15 mins [30].

Roger's Group and Huang's Group have made outstanding contribution to the

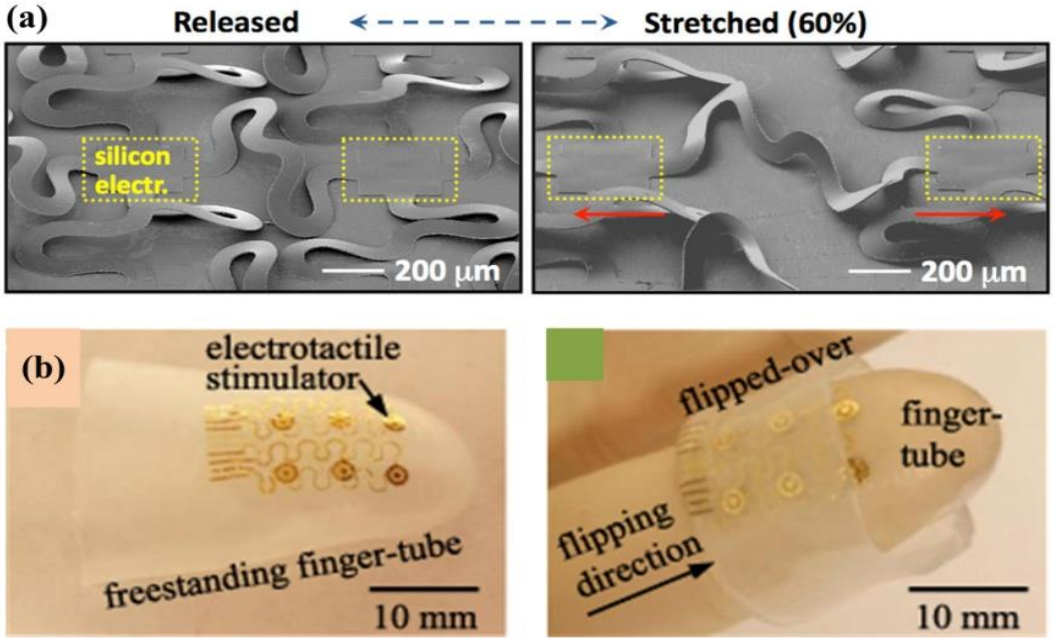

Fig. 1.9 (a) Flexibility achieved of traditional materials by wavy structure; (b) Finger-shaped flexible tactile sensor made by Si and Au based materials

flexible and stretchable sensor development during the last few years as well. Several flexible devices which made by tranditional materials like metal and silicone based materials are reported. The wavy structure showed in Fig1.8(a) enable the tranditional inorganic conductive materials to extend, deform without fracture and damage [31]. Based on this, they developed a finger-tube shaped flexible sensor which can be wore on finger tightly, but it's noted that the applied pressure did have considerable effects on the stretchability for different orientation, which may led to the dispute of the conductor, thus this is not considered as a primary solution for pressure detection.

In 2012, McApline and coworkers developed a resistive graphene sensor that was printed on a bio-resorbable silk substrate. It's size is similar with finger nail, they showed the sensor could be attached on complex surfaces like tooth enamel, muscle tissue by dissolving the silk substrate. It consist of an inductor and interdigitated capacitive electrodes made by graphene and integrated on thin silk film. Function the

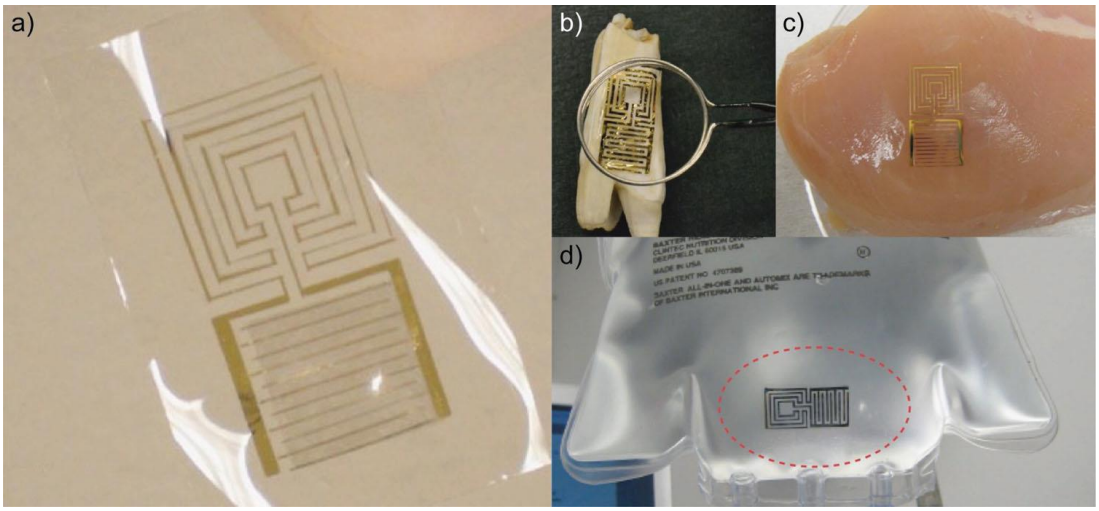

Fig. 1.10 Biodegradable graphene nanosensor (a) sensor consisting of an inductor and interdigitated capacitive electrodes integrated onto a graphene/ silk fi lm. Graphene nanosensor transferred onto (b) a cow molar,(c) muscle tissue, and (d) an intravenous bag.

graphene surface with antimicrobial peptides enables it to detect Escherichia coli bacterium[32].

Recently, Hyunhyub Ko and coworkers designed a piezoresistive interlocked micro dome arrays that imitating the epidermal-dermal ridges in human skin, the unique geometry of interlocked structure enables the differentiation of various mechanical stimuli, since the array will exhibit different levels of deformation depending on the applied force direction, which enables the sensor detect the normal, shear, bending, and twisting forces [33].

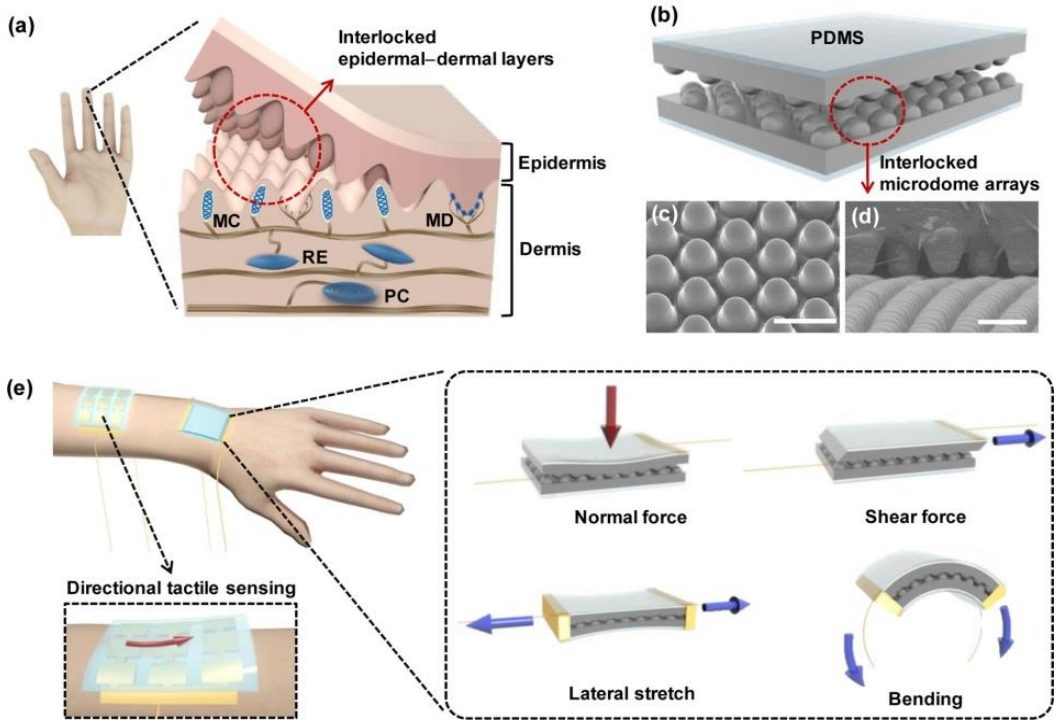

Fig. 1.11 (a)-(e) CNT-PDMS based interlock structure e-skin by Ko's goup

There're several different types of principle for flexible tactile sensor design. Cotton's group firstly presented a stretchable and multifunctional capacitive sensor made of gold thin films embedded in silicone rubber, which showed fair ability to

bend, fold and stretch, while the poor adhesion between gold films and silicone substrate made the integration of tactile sensor difficult [34]. Araki's group proposed a tactile sensor made of flexible and stretchable silicone rubber utilizing static electricity and an electrostatic induction phenomenon to detect contact with the environment. However, the sensor showed lack of resolution of different pressure [35]. Ohmura and co-workers designed a conformable and scalable tactile senor skin, the skin is organized as a network of self-contained modules consisting of tiny pressure-sensitive elements which communicate through a serial bus. Although it is possible to adjust the coverage area by adding or removing modules, the substrate on

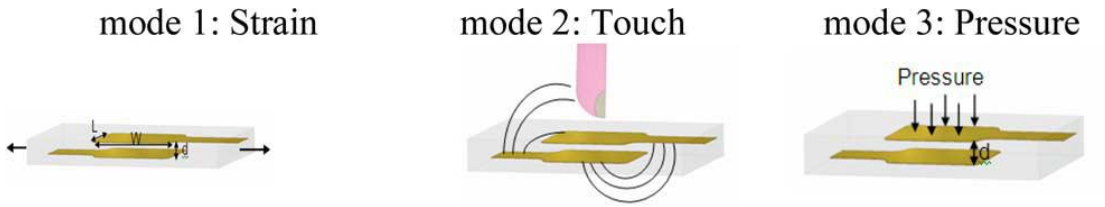

Fig. 1.12 Capacitive sensor mode made by gold thin film/PDMS by Cotton et al.

which the modules are mounted lacks stretchability [36].

The key challenge to make the entire sensor array structure stretchable and conformable is the stretchable inter-connections, various materials and structures have been developed to realize it, such as wavy thin metals [37], silver flakes embedded elastomers [38], transparent graphene films [39], carbon nanotube-based composites [6], etc. However, there're some common limitations associated with these designs like low conductivity, poor stretchability, resistance increase with applied strain, as well as poor adhesion between the substrate and patterned conductors.

Someya's group reported a 16 by 16 organic transistor matrix to detect physical

stimuli, which applied resistive mechanism to sense the change of pressure, is built with PEN base and gold electrodes, and 28μm PVDF thin film as transducer. The device didn't exhibit any significant variation in electric property under above 50% stretch [40]. Considering the inherent advantages of the resistive sensor array such as less electronics requirements, ease of manufacture and integration, less susceptibility to noise and therefore applicable to mesh configurations, the piezoresistive principle is selected in our tactile sensor design.

Fig. 1.13 T.Someya's group designed an Ag electrode coated transistor interconnected by elastic conductors on PDMS sheet which can sustain some biaxial stretching

Since the demand for the versality of e-skins are growing larger, more efforts have been put for investigating the new desired properties like biocompatiblity/biodegradability, self-healing, temperature sensitivity, self-powering and so on. However, how to make these sensors with large area and remain well function under multiaxial deformation is still a stubborn issue and few related work has been reported these years.

1.3 Goal and Contents of Current Research Work

Based on the current e-skin development scenerio mentioned above, the goal of our project is to develop a highly flexible and stretchable, mostly transparency, light,

wide range tactile sensor array. Our study includes:

(1) The fabrication and testing of stretchable electrodes. Expectation:

    1) Remain low resistance at both uniaxial and muli-axial deformation up to 60%, fuction under the severe condition(100% and above).

    2) Research and compare the effect of different metalization routines for the electrode.

(2) The lamination and assembly of the electrode and piezoresistive sensels. Expectation:

    1) Evaluate the contact performance between electrode layer and piezoresistive materials after different metalization routines.

    2) Optimizing the assembly propotype to enhance the conducting performance and reduce the abrasion between layers, to realize long-term accuracy and repeatable use stability.

(3) Implement the tactile pressure sensing under muliti-axial, especially bending condition. Expectation:

    1) Utilize different types of intrisinc flexible materials as matrix to provide better conformability for the whole sensor array, engineer the embedment of sensels to ensure the sensing layer have similar stretchability as well.

    2) Enlarge the detection range of our e-skin, which imply the sensing and signal reception component of our sensor system must be in good correspondence.

(4) Integrate the sensor with medical equipment, in our study, we attached our flexible tactile sensor around the colonoscope to measure the contact pressure on

the tube. Expectation:

1) Introduce the signal from the tubular shaped sensor to signal reception circuit properly, with neatly and nicely wire layout.
2) Realize initial implementation of real-time pressure monitoring inside colon-simulator, which will totally demonstrate the feasiblity of our high flexible, high sensitivity sensor array to help address the knotty issue in colonscopy mentioned in last section.

1.4 Structure of Dissertation

In correspondence to the contents of our research work mentioned above, the structure of this dissertation is:

Chapter 1: Introduction. Introduce the originality of our work, overview of the development, progress and concerns about flexible tactile sensor.

Chapter 2: Design of the tactile sensor, property of the materials used as matrix and electrodes in our sensor fabrication. Test for the stretchable electrodes with different base materials and different metalization routines. Information about data acquistion system.

Chapter 3: Investigation of our sensor's performance under bending deformation(with and without external pressure). Evaluate and eliminate the systematic error for our sensor system.

Chapter 4: The integration of our sensor system with the colonoscopy, real-time pressure dectation realization.

Chapter 5: Conclusion and prospects of automation for our sensor fabrication.

CHAPTER 2

Design of Tactile Sensor System

In this chapter, we describe the structure of our tactile sensor, two different routines of fabricating the high flexible electrode layers are presented, property of each component of the sensor were concluded. In addition, four series of metallization methods were designed to further enhance the conductivity, fatigue tests were carried out as well. The remaining parts are about the designing of scanning circuit, data acquisition system, and the assembly of the sensor.

2.1 Structure of Tactile Sensor

Most of the tactile sensors are composed of two major parts: pressure detection array and signal process unit. While the structure of pressure detection array and property of components determine the sensitivity and the accuracy of the sensor, the optimization of signal process unit help improve the efficiency of detection and reduce error. In this project, we developed a three layer sensor array containing 8 by 8 sensor elements, its spatial resolution is 1 element per $9mm^2$ area. The upper and lower layers are silicone thin films embedded with a kind of flexible conducting strip, silver nanowire. The middle layer is a silicone thin film patterned with piezo-resistive rubber disks.

The schematic diagram of the proposed tactile pressure sensor array is shown in Fig.2.1. To realize high flexibility and stretchability of sensor array structure, two types of silicone, Polydimethylsiloxane(PDMS) and Dragon Skin® are selected to build the sensor respectively. The AgNWs/PDMS(Dragon Skin) conductor strips are

used as stretchable interconnections and sensing electrodes. The thin PDMS(DS)

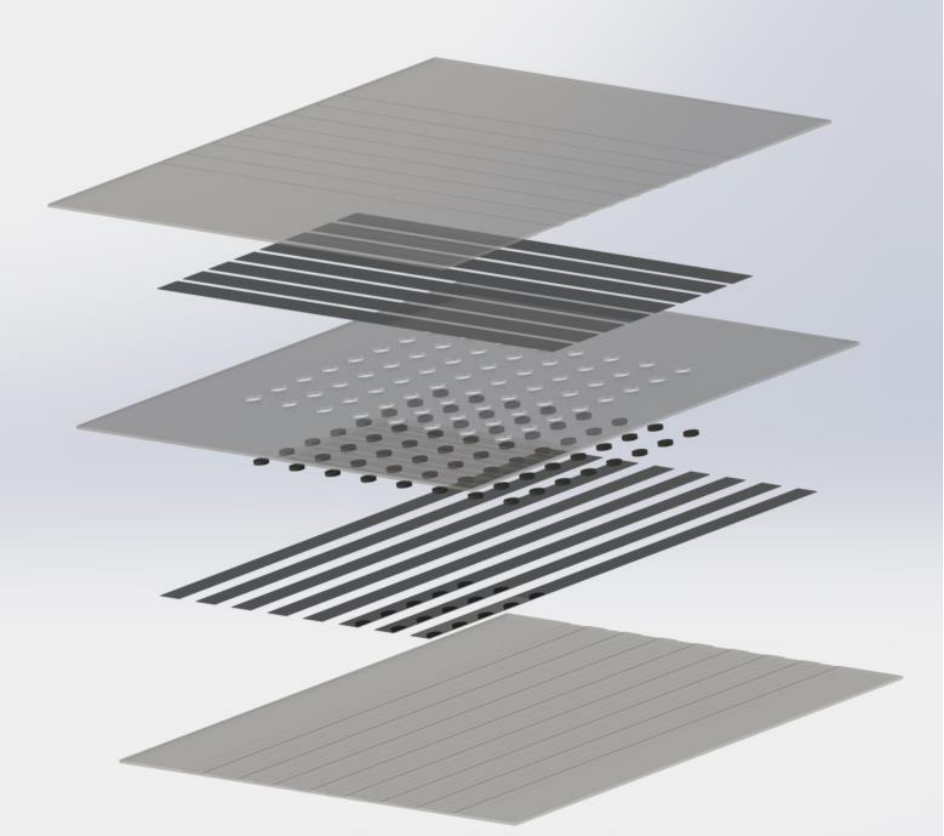

Fig. 2.1 Diagram of sensor layers (1) PDMS outer layer (68 × 72 ×0.4 mm), (2) PDMS middle layer w/ 64- 2.5mm dia. holes (68 ×72 ×0.4mm), (3) 64-graphite foam piezoresistive sells (2mm dia. × 0.45mm (4) AgNWs (3.5 × 72 or 68 by orientation ×0.1 mm), (5) PDMS outer layer (72 ×68 ×0.4mm).

structure provides the sensor array compliance and stretchability, the conductive elastomer is used as the piezo-resistive elements. They are cylindrical in shape and embedded in the pre-molded holes of PDMS thin film. The PDMS thin film functions as insulated springs. On one hand, it holds the piezoresistive elements together and improves the stretchability of the middle layer. On the other hand, its isolation among piezoresistive elements eliminates the crosstalk.

The sensing layer is sandwiched between two PDMS thin films, each of which brings rows of parallel AgNWs/PDMS conductive strips in contact with the

piezoresistive elements. The conductive strips in the top and bottom layers are placed orthogonal to each other. Together with the sensing elements in the middle layer, a matrix of sensels is built up. In the matrix, the sensing area of each sensel is one portion of the cylinder-shaped piezoresistive element at the crossing of the upper and bottom conductive strips.

When a pressure is applied on the tactile sensor array the deformation of a cylinder-shaped piezoresistive element leads to the resistance change of the sensel. Thus pressure can be obtained through the measurement of the sensor cell's resistance value.

2.2 Components of Sensor Arrays

The flexible sensor array is basically made of three components: a silicone base works as substrate, a flexible conducting material as electrode, and piezo-electric materials for pressure detection elements. In this project, we employed two different types of silicone individually, and applied silver nanowire as the conducting electrode. For pressure detection, a carbon based piezo-resistive rubber is selected. We will introduce each of them in the following paragraph.

2.2.1 PDMS

Polydimethylsiloxane(PDMS) is known as a commercially available polymeric organosilicon rubber. Being an elastomeric silicone, PDMS is inexpensive, flexible, and optically trans-parent down to 230 nm, which make it well suited for a wide range of applications such as mechanical interconnection layer between two silicon wafers, ion selective membranes on ISFETs and spring material in accelerometers [41]. Further properties of PDMS include the low change in the shear elastic modulus

versus temperature, impermeable to water, nontoxic to cells, and permeable to gases [42]. Because of its intrinsic advantages like clean room processability, low curing

Fig. 2.2 PDMS silicone(Sylgard 184 silicone elastomer base) from Dow Corning®

temperature, high flexibility, the possibility to change its functional groups and easy to be fabricated and bonded to other surfaces [43], PDMS has been the most

Table 2-1 Major properties of PDMS elastomer

Property	Value
Density	0.93kg/m^3
Young's Modulus	~1Mpa
Poisson ratio	0.5
Tensile strength	2.24Mpa
Specific heat	1.46kJ/kg K
Thermal conductivity	0.15 W/m K
Dielectric constant	2.3-2.8
Refractive index	1.4
Conductivity	$4\times10^{13}\Omega$m
Permeability	$0.6\times10^{6}cm^3/g$
Adhesion with SiO_2	Fairly good
Biocompatibility	No harm to human body
Hydrophobicity	High, contact angle 90-120 degree

popular base for micro-machined mechanical and chemical sensors [44].

The Dow Corning 184 Silicone Elastomer® is a two component, room temperature and heat curing encapsulant whose properties are already thoroughly studied and tested. It has been proved that this material can provide a good flowability, dielectric property and moisture protection for sensitive electronics parts.The structural and surface properties of PDMS Sylgard®184 will be the most optimal choice to the design, fabrication, and development of PDMS micro- and nanostructures for biomedical applications among the whole PDMS series.

In our research, this kind of PDMS was applied as the one type of the flexible base for our flexible sensor array. Its properties are listed in table 2-1.

2.2.2 Dragon Skin

Dragon skin® silicones are high performance platinum cure liquid silicone compounds supplied by Smooth-On®, it's applicable for a variety of applications from life-casting, medical simulation to all kinds of model making. Being proved as skin-safe silicone, Dragon skin has taken the spotlight in movie special effects and medical prosthetics. Considering the superior mechanical property, wide service temperature range, super low long-term shrinkage, Dragon Skin can be the most ideal matrix material for our high stretchable and flexible tactile sensor. So far, there're only a few of actuators reported for using Dragon Skin as matrixes, the property of this new type silicone is barely studied. In this project, the Dragon Skin 10 medium kit is chosen. By mixing the two parts with the ratio of 1:1, up to 475psi tensile strength and 500% elongation could be achieved.

Fig. 2.3 Dragon Skin® Platinum Cure kit 10 medium

2.2.3 Silver Nanowire

Nanowire is a quasi-one-dimensional nanostructure with the diameter of the order between 1~100 nm (10^{-9}meters) [45]. At this scale, quantum mechanical effects are quite obvious and important, which coin the term "quantum wires". There are different types of nanowires including insulating (SiO_2,TiO_2), superconducting,

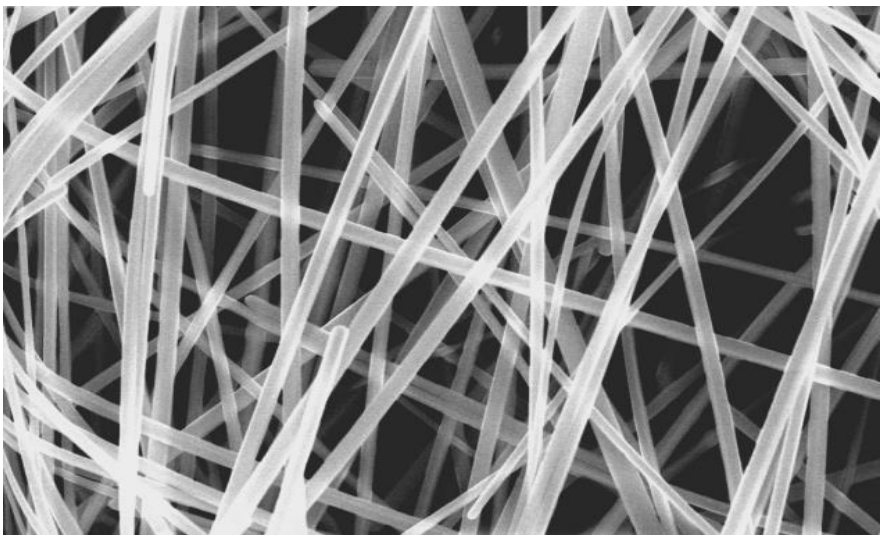

Fig. 2.4 SEM Picture of SLV-NW-90 AgNW from blue nano®

metallic (Ni,Pt,Ag) and semiconducting (Si,InP,GaN,etc). Among these types, the metal nanowires reveal new physical and chemical phenomena that are a direct consequence of their size, shape, and reduced dimensionality, these phenomena enable genuinely new kind of device, from high density perpendicular data storage to nano-sensors, from high-sensitivity nano-electrodes to meta-materials, and so on [46].Namely, metal nanowires have been becoming integral functional components for lots of burgeoning applications. Among metal nanowires, silver-nanowires(AgNWs) have already been demonstrated to provide high DC to optical conductivity ratio, which is the crucial merit of nanostructure conductors [47]. Apart from this, silver nanowires revealed following exciting advancements: firstly, routinely synthesized high aspect-ratio AgNWs bring about great performance improvement for AgNWs based transparent electrodes. Secondly, a kind of rod coating technique for roll to roll deposition of AgNWs has been realized to make precisely pattern possible. Thirdly, the junction resistance between AgNW-AgNW can be easily reduced by proper annealing method. Moreover, the adhesion and bending stability, and chemical stability of AgNWs are able to be controlled by a variety of modes according to certain studies [48, 49]. All those attractive features favor AgNWs unique superiority over traditional conducting thin films like ITO and pervasively studied carbon nanotubes(CNT) in recent years.

Philip Lee presented highly stretchable and highly conductive metal electrodes with the newly developed long AgNWs(＞500μm) embedded in pre-strained Ecoflex, which showed significantly enhanced mechanical compliance over CNTs, graphene,

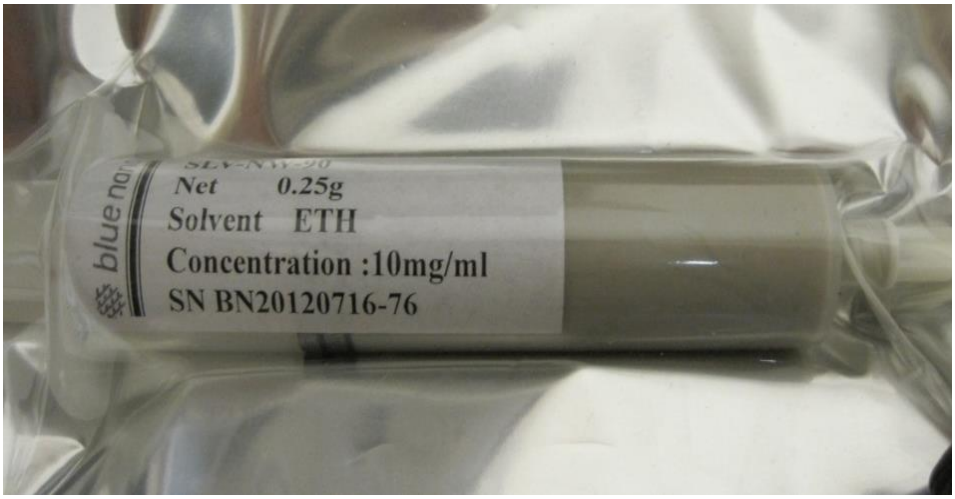

Fig. 2.5 SLV-NW-90 AgNW pack from Blue Nano®

and other metal nanostructured conductors [50]. Recently, JY Woo reported a AgNWs/CNT hybrid conductor that shows similar mechanical and conducting performance without the need to pre-strain of Ecoflex, which further demonstrate the suitability for AgNWs working as interconnector applications in flexible electronics[51]. In our work, the AgNWs are embedded on flexible substrate like PDMS or Dragon skin as conducting strips with the width of 3mm.

2.2.4 Pressure Sensitive Electric Conductive Elastomer

For sensing element, a kind of piezo-resistive material was chosen, it can respond to the resistivity changes due to mechanical deformations or applied pressure [52]. Typical piezo-resistive sensors include conductive elastomers, carbonizing organic fibers and so on [53]. Conductive elastomers are elastic materials(e.g, polymers) infused with conductive powders like metal [54] and carbon black [55, 56], or conductive films like nanotubes [38, 57] or nanosheets [58], they are able to undergo large deformations, and at the same time show the change in resistivity. With their

Fig. 2.6 Conductive elastomer CS57-7RSC

remarkable flexibility, high reliability and relatively high cost-efficiency, piezo-resistive rubber fits for the functionality needed in our e-skin sensor perfectly. The technique of fabricating sheet-type tactile conductive rubber had been developed and continuously improved within the past decades [59], in our research, a kind of sheet-type electric conductive elastomer CS57-7RSC(PCR Technical, Japan) was chosen, it has unique property in that it conducts electric current when compressed and acts as an insulator when the pressure is released [26, 60]. This material is a

composite of an elastomer and specially treated carbon particles, and is available in gray-black flexible sheet form, 0.5mm in thickness.

Table 2-2 Physical property of CS57-7RSC

Color	Gray-black
Tensile Strength	1.86Mpa
Elongation at break	220%
100% modulus	0.86Mpa
Tear Resistance	7kN/m
Hardness in Durometer	50

2.3 Fabrication and Test of Stretchable Electrode

To realize high sensitivity and versatility sensing for the e-skin, maintain good conductivity under large deformation is the key requirement for the stretchable electrodes. The elastic nature of siloxane-based elastomers mentioned above can enable different types of embedment for flexible conductive materials. Over the last few years, PDMS thin films have been the most favorable substrates in the fabrication of flexible electronic devices due to their good elasticity and outstanding biocompatibility. However, this kind of thin film usually suffers from poor resistance to tearing and insufficient compliance to curved surfaces, which limits their applications. So in order to fabricate high performance three-dimensionally mountable tactile sensor arrays, we developed the mechanically compliant electrodes by patterning AgNW trace in strip-style on Dragon Skin® (DS) substrates instead of PDMS, and compared with those with PDMS base. In addition, to achieve precise control of the thickness of each sensor layer in order to realize the standardized and uniform fabrication flow line, a new preparation process of paper spacing extrusion is developed and applied here. Furthermore, to improve the conductivity of stretchable

electrodes, two types of Physical Vapor Deposition (PVD) processes, sputtering and electronic beam evaporation, were applied to coat a gold layer on the electrode strips. Moreover, the adhesion effects of different interlayers (Titanium and Chrome) between the gold trace layer and the AgNWs surface were studied as well. Once assembled, the DS/AgNWs electrode thin films would be subjected to fatigue testing, to evaluate their ability to perform well in real applications.

2.3.1 Fabrication of Flexible Electrode by Spin Coating

The following steps have been used to fabricate the proposed PDMS/AgNWs and the DS/AgNWs stretchable electrode thin films, thin and uniform films achieved by spinning coating:

#1: Some liquid PDMS (Dow Corning Sylgard 184, ratio of base to cross-linker is 10:1 by mass) was dispersed on 5 inch silicon wafers by spin coating (spin parameters

Table 2-3 Parameters for spin coating in Steps #1 and #4

Process Steps	Parameters		
	Acceleration	**Speed**	**Time**
Spread	200rpm/s	800rpm	10s
Spin	250rpm/s	1000rpm	30s

are shown in Table 1), and was thermally cured in an oven at 65℃ for 12 hours to make molds for AgNWs networks of the electrodes.

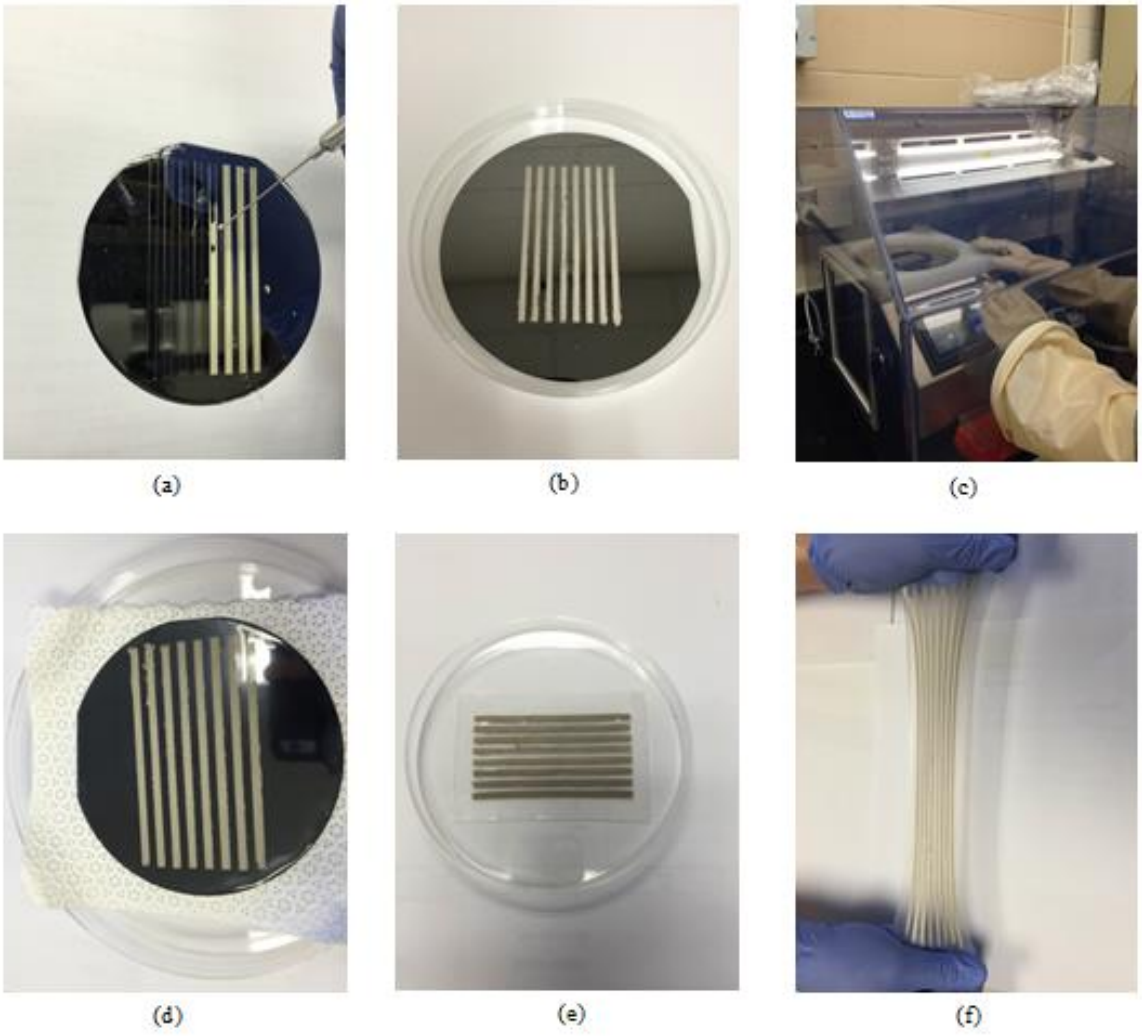

Fig. 2.7 Fabrication procedure of stretchable electrodes (a) Patterning AgNWs conductive strips in a removable PDMS mold; (b) The parallel patterned AgNWs strips; (c) Mixed PDMS (or DS) dispersed on AgNWs by spin coating in a glove box; (d) Thin and uniform electrode thin film after spin coating; (e) The electrode thin film was peeled off from a silicon wafer; (f) The DS based electrode thin film can be stretched over 150%.

#2: AgNWs (Blue Nano, 10mg/ml) were dried in these PDMS mold on the silicon wafers by a syringe, forming the eight parallel strips of AgNWs networks (Fig. 2.7a).

#3: As the AgNWs dried, the PDMS mold was removed (Fig. 2.7b) and the remaining AgNWs strips are patterned.

#4: Some liquid PDMS was mixed, degassed and poured over the AgNWs strips, and dispersed by spin coating again (Fig. 2.7d). The same procedure was repeated when

we made the thin films with DS as the substrates.

#5: Finally, the whole structure was thermally cured for 12 hours, after this, the PDMS (Dragon Skin) electrode thin film was peeled off from the silicon wafer carefully (Fig. 2.7e).

2.3.2 Fabrication of Flexible Electrode by Controlled Spacing Extrusion

Spin coating is the most commonly used procedure to deposit thin, uniform film. Usually with higher angular speed, thinner film can be obtained. As we demonstrated above, nice and uniform electrode layers are fabricated with spin coater. However, this process is basically an empirical method, it's impossible to precisely control the thickness of the layer. In order to compass the object of controllable fabrication for the whole sensor array, we come up with a new approach by extrusion. Here are the detailed steps of this approach:

#1: Some liquid PDMS (Dow Corning Sylgard 184, ratio of base to cross-linker is 10:1 by mass) was dispersed on 5 inch silicon wafers by spin coating, and was thermally cured in an oven at 65℃ for 12 hours to make removable molds for AgNWs networks of the electrodes (Fig. 2.8a).

#2: Removable PDMS mold was placed on a glass plate, and AgNWs (Blue Nano, 10mg/ml) were dried in these PDMS mold on the silicon wafers by a syringe, forming the eight parallel strips of AgNWs networks.

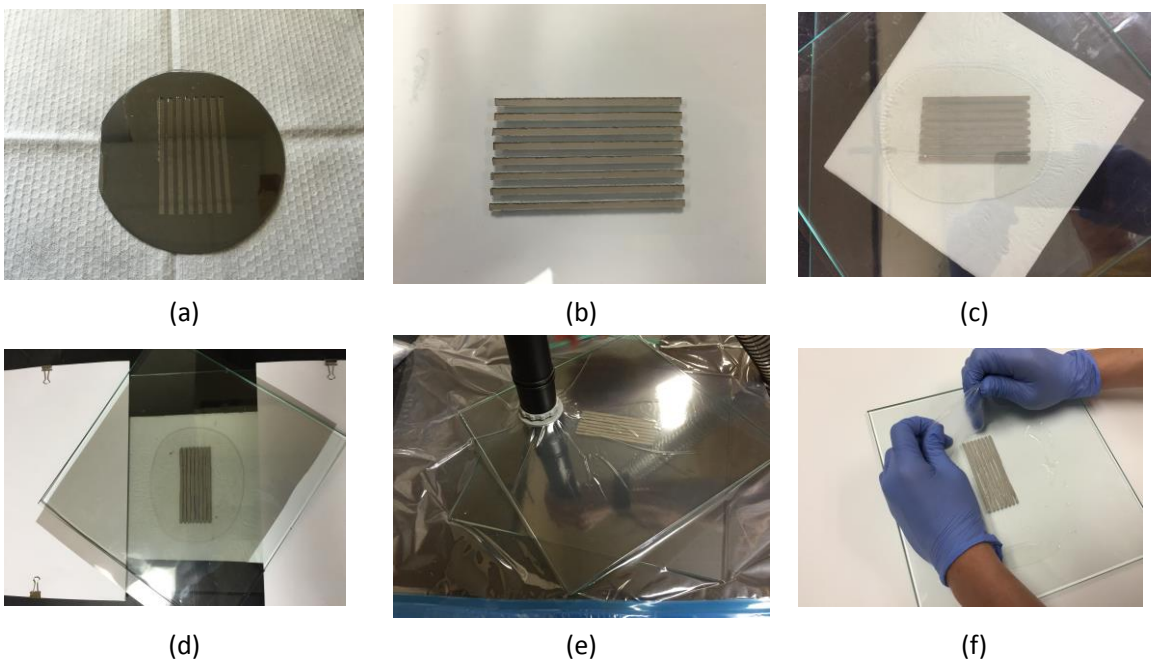

Fig. 2.8 Fabrication of electrode layer by extrusion (a) make removable molds for patterning AgNW strips; (b) parallel patterned AgNW Strips on glass plate; (c) another glass plate cover on top of uncured silicone; (d) paper spacing extrusion; (e) degas in a vacuum bag; (f) peel off the ultra-thin electrode layer

#3: As the AgNWs dried, the PDMS mold was removed (Fig. 2.8b) and the remaining AgNWs strips were patterned.

#4: Some liquid DS(Smooth-on medium kit) was mixed and poured over the AgNWs strips, followed by another glass plate covered on top of it(Fig. 2.8c).

#5: Two pieces of paper was inserted at side gaps, and pressure was applied on the top glass plate to extrude the liquid silicone till the electrode layer reaches the sample thickness as the spacing paper (Fig. 2.8d).

#6: The uncured electrode layer was put into a vacuum bag with the two glass plates, for degassing and curing for 4 hours (Fig. 2.8e).

#7: Ultra-thin DS electrode thin film was peeled off from the glass plate carefully (Fig. 2.8f).

2.3.3 Resistance Measurement after Metalization and Stretchability Comparison

Following the fabrication process, the stretchable electrode thin films were categorized into 4 groups for further metallization process. A sputtering system from AJA International, Inc. and an evaporation system from CHA Industries, Inc. were utilized to coat a thin gold layer on different groups of the AgNWs conducting strips. Titanium (Ti) and chrome (Cr) were applied as the adhesion layer for the deposition

Table 2-4 Parameters for different PVD processes

No.	PVD Process	Metalized layer	Parameters		
			Chamber Pressure	Depo-sition Rate	Total Time
#1	E-beam evaporation	Ti(10nm)+ Au(50nm)	1.5×10^{-6} Tor	0.2nm/s	300s
#2		Cr(10nm)+ Au(50nm)			
#3	Sputtering	Ti(10nm)+ Au(50nm)	1.0×10^{-5} Tor	0.25nm/s	240s
#4		Cr(10nm)+ Au(50nm)			

of gold layer. Ti and Cr have been commonly used in assembling different kinds of metal powders with silicon-rubber thin films to form a multilayer structure in electrical contact relays, as an adhesion/diffusion media [61, 62]. They can also introduce considerably adhesion improvement for gold powers. The applied parameters in our process are shown in table 2-4.

A 10nm interlayer was achieved in each of the sample groups, and a 50 nm gold layer was coated in succession as shown in Fig. 2.9(a). The measurements for stretchable electrodes were shown in Fig. 2.9(b) and Fig. 2.9(c). Resistances of each group are listed in Table 2-5. At least 16 different conducting strips have been

measured for each PVD process to get the reliable values.

Table 2-5 Resistances of the stretchable electrodes after different metallization routines

No.	Conductor Strip	Resistance (Ω/1mm)
#0	AgNWs	0.178
#1	AgNWs/Ti/Au by E-beam	0.125
#2	AgNWs/Cr/Au by E-beam	0.084
#3	AgNWs/Ti/Au by sputtering	0.157
#4	AgNWs/Cr/Au by sputtering	0.103

From the data shown above, it's noted that the resistance of group #2 strips, which were coated with a 50nm gold thin layer with chrome as interlayer by E-beam, is the smallest among all the strips with and without PVD processing. There are mainly two reasons explaining this: one is that the chrome has higher inter-diffusion rate with AgNWs, and provides better adhesion force for the AgNWs to contact with each other in these samples. Another reason is that the E-beam evaporation permits more direct energy transfer to the source during heating than sputtering; due to the higher vacuum degree achieved, the E-beam can bring purer evaporated material to the substrate, thus the electrode processed by E-beam shows better conductivity than those by sputtering.

From Fig. 2.9(d) and Fig. 2.9(e), it is also observed that although the PDMS-based electrode substrate is thin, it could not be conformably mounted to a curved surface and the two sides of the PDMS/AgNWs thin film tilt up on the tennis ball, while the DS-based electrode thin film could be wrapped around a tennis ball

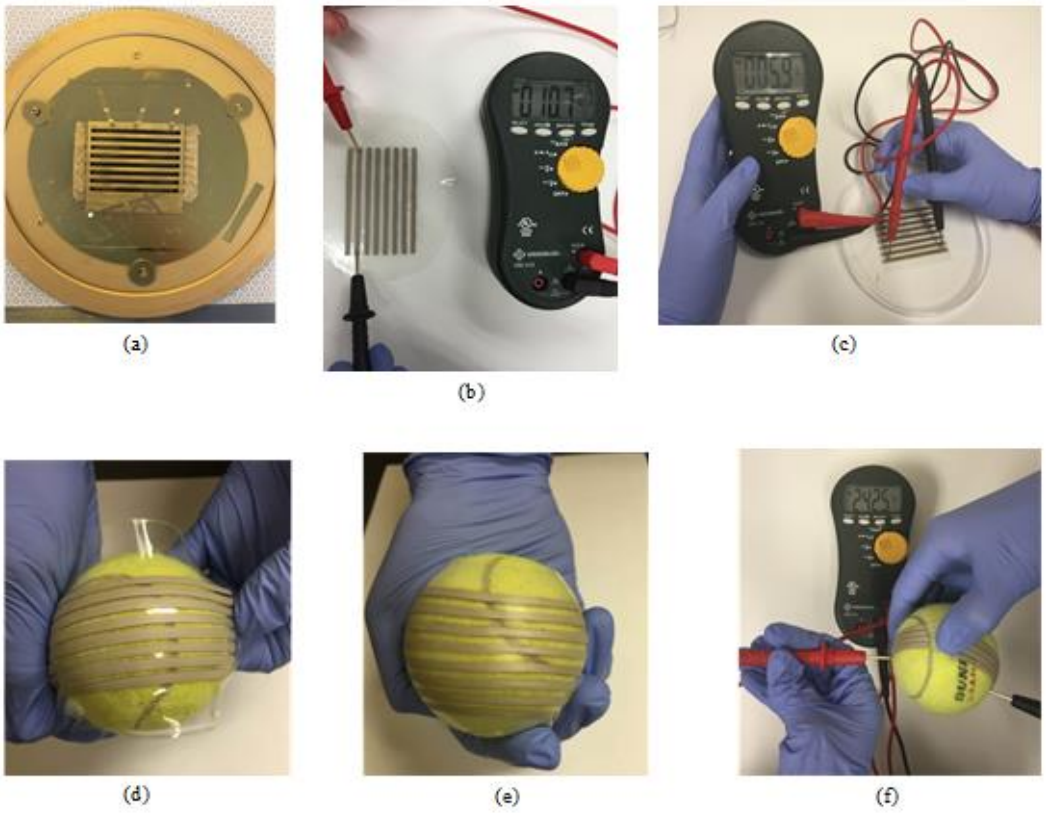

Fig. 2.9 Electrodes test after metalization (a) Stretchable electrodes flipped under a mask on a sample holder for PVD processes; (b) Resistance of a 60mm AgNWs conducting strip is about 11Ω; (c) Resistance of a 80mm AgNWs/Cr/Au(E-beam deposited) conducting strip is below 6Ω; (d) A tennis ball is wrapped by an AgNWs/PDMS electrode thin film; (e) A tennis ball is tightly wrapped by an AgNWs/DS electrode thin film; (f) The AgNWs/DS electrode thin film can keep low resistance under large 3D deformation.

tightly and conformably. In Fig. 2.9(f), a 80mm long AgNWs/DS electrode thin film can be wrapped around a tennis ball (r = 33mm) with elongation of nearly 160% and still keep a resistance of 2.2Ω/1mm, which is on the top level of any kinds of stretchable electrodes under large deformation.

2.3.4 Fatigue Test

In the actual application, the stretchable thin films with conductive strips will be used in a working condition with repeated stretching and relaxing motions. Thus the fatigue property of this kind of thin films is one of the important factors which will influence its applicability. In the following, the tests to demonstrate the capability of

the thin films to withstand repeated deformation were carried out. Its conductivity after the repeated motion was measured to evaluate its anti-fatigue property. The

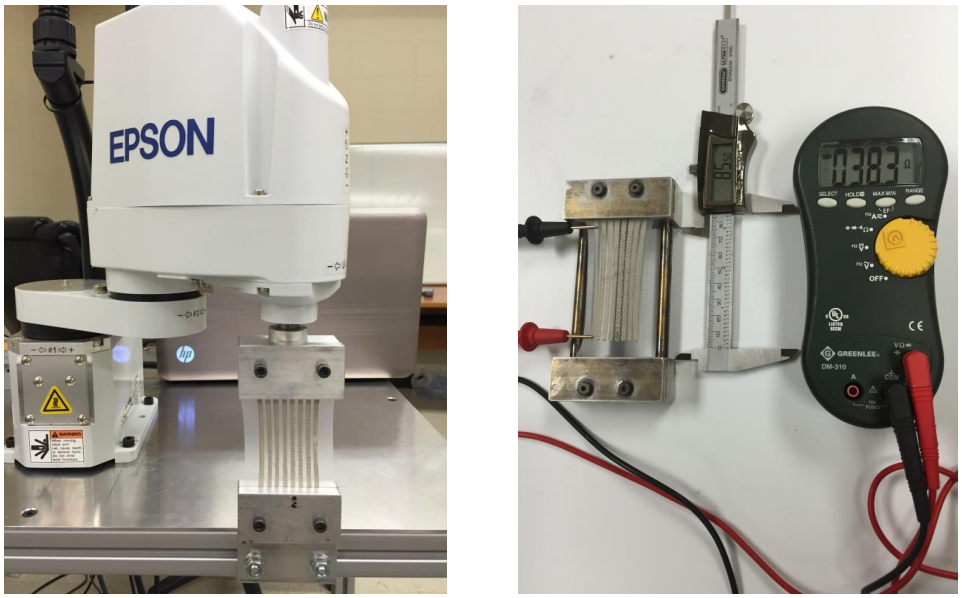

Fig. 2.10 Tensile testing stage after fatigure test

experimental setup is shown in Fig. 2.10. The main testing component is a piece of DS/AgNWs thin film with 8 conductive strips. One side of the thin film was clamped to the end-effector of an EPSON robot and the other side was fixed to the table using a table mounted clamp. The end-effector of the robot was then controlled to move repeatedly to generate repeated stretching and relaxing motion. After the DS/AgNWs electrode thin film was stretched and relaxed for certain times, such as 1 time, 3 times, 5 times and 100 times, it was taken off from the robot and mounted to a tensile testing stage for measurements as shown in Fig. 2.11. On this stage, the resistances of the conductive strips on the film were measured at certain strain rate from 0% to 70%, such as 5%, 10%, 15%, etc. The results measured in resistances per mm were shown in Fig. 2.11.

From results shown in Fig. 2.11, a linear relationship between the increase of the

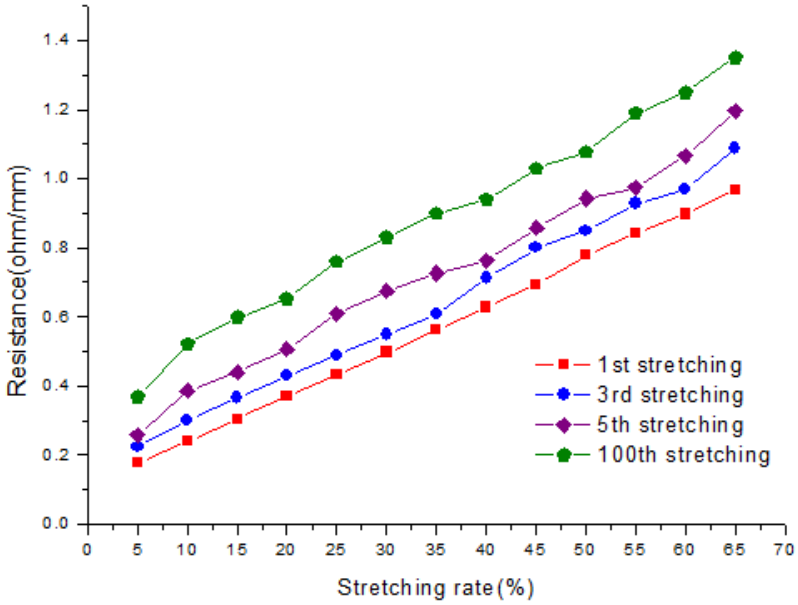

Fig. 2.11 Resistance of an AgNW/Dragon Skin stretchable conductive strip as a function of tensile strain at different stretching cycles

resistance per millimeter and the increase of the strain rate can be observed. It can also be observed that the more times the thin film was stretched, the bigger the thin film's resistance was. There was an average overall of 12.5% increase in resistance from the first to third stretching, 14.9% increase after the 5^{th} stretching, and 24.8% following the 100^{th} stretching. After around 100 times stretching, the resistance of the thin film did not increase any more. This is to say that the DS/AgNWs electrodes can withstand repeated stretching and maintain high conductivity when working in a reasonable range of strain (0% - 70%).

From this study about different types of stretchable electrodes, it is noted DS base with AgNWs aligned on it will provide highest stretchability, and facilitate our design for multi-axis deformable tactile sensors best. In addition, e-beam deposited a

thin gold film with chrome as interlayer will help the DS/AgNWs electrode achieve unprecedented high conductivity. Since large area e-skin will be fabricated in this project, the metallization process is not obligatory in this case as multi-pass AgNWs have already provided sufficient conductivity.

2.4 The Design of Scanning Circuit

Figure. 2.12 shows the integrated system which includes a sensor array, a scanning circuitry, and PC. For signal scanning, a constant voltage is applied to the

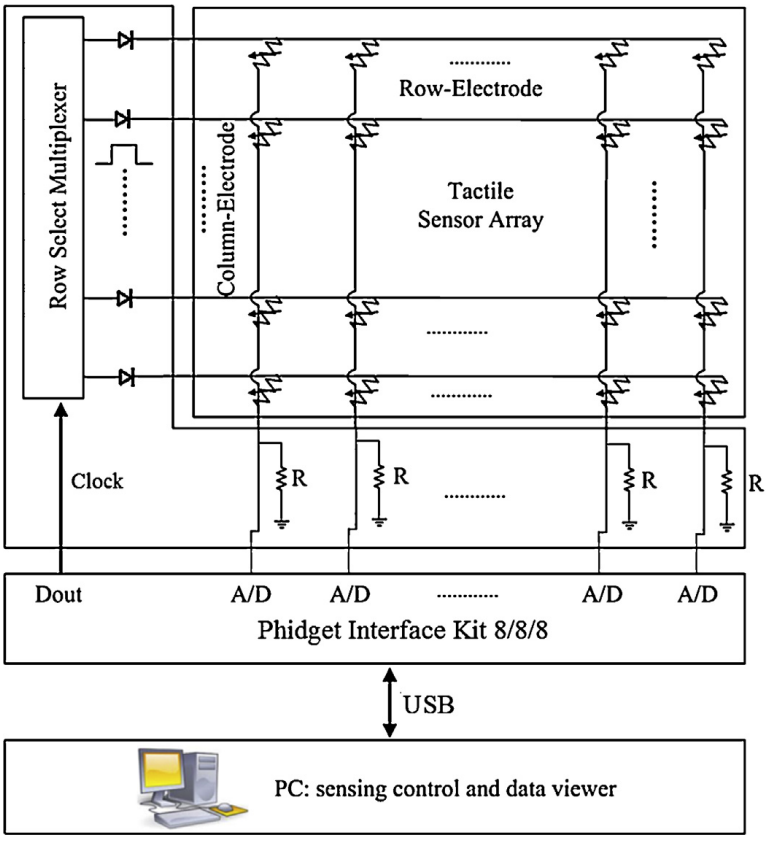

Fig. 2.12 Schematic of tactile array system

row that wa selected, and other rows are set to zero voltage. In the vertical direction, operational amplifiers were connected to all of the columns, and all of the columns

are brought to zero voltage. By doing this, the error in the measurement due to leak resistance between electrodes can be excluded. The change in current flowing through each sensing element can be detected by the current-to-voltage converter. The scanned output voltages of tactile sensor array are transferred to analog-to-digital(AD) converter of an MCU. The PC is used to adjust the gain of each sensor element and the offset due to the initial pressure occurring when the sensor is assembled, as well as display the pressure distribution image.

2.5 Main Components of Data Acquisition System

There are basically four major devices in our pressure detection system:

(1) The silicone based tactile sensor(as shown in Fig. 2.1)

(2) Microcontroller-Parallax BS2p40

The I/O pin P0-P7 of the microcontroller connected to each column of the sensor array to control the output and get the data acquisition system run. Port VIN(Unregulated power in) and VSS(System ground) are connected with the power supply.

(3) Power Supply

BK Precision 1670A, which provides the 5V power needed in our system.

(4) PhidgetInterfaceKit 8/8/8 Data Acquisition Cards

The analog input of this Data Acquisition Cards is used to measure the pressure. Wires introduced from the tactile sensor can be plugged directly into the board, and the sampling rates can be set from 1ms up to 1000ms. In our case, the graphicuser interface(GUI) on the computer is based on Visual Basic 6.0. It will realize the features of relating the pressure on each sensel to the darkness of color block on the computer interface.

Table 2-6 Stamp specification of BS2p40

Package	40-pin DIP
Package Size	2.1"×0.6"×0.4"
Environment	0°-70℃(32°-158℉)
Microcontroller	Parallax SX48
Processor Speed	20 MHZ Turbo
Program Execution Speed	~12,000 instructions/sec.
RAM Size	38 Bytes(12 I/O, 26 Variable)
Scratch Pad RAM	128 Bytes
EEPROM Size	8×2K Bytes, ~4,000 inst.
Number of I//O pins	32+2 Dedicated Serial
Voltage Requirements	5-12 vdc
Current Draw@5V	40 mA Run/ 350μA Sleep
Source/Sink Current per I/O	30 mA/30 mA
Source/Sink Current per unit	60 mA/ 60 mA per 8 I/O pins
PBASIC Commands	61
PC Programming Interface	Serial(9600 baud)
Windows Text Editor	Stampw.exe(v1.1 and up)

2.6 Integration of Sensor System

With insights of all components and the ultra-thin, high flexible tactile sensor layers obtained by the way concluded in chapter 2.3. We performed the following steps to fabricate the middle layer and assemble the proposed tactile pressure sensor array:

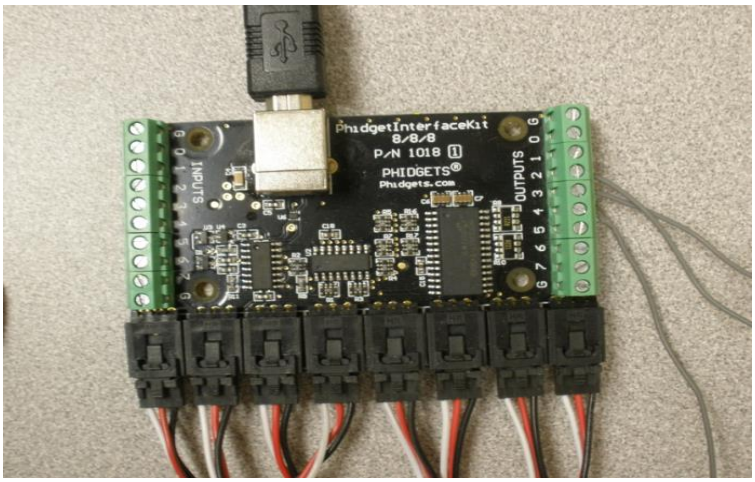

Fig. 2.13 Phidget InterfaceKit 8/8/8 Data Acquisition Cards

#1: For the middle layer, a SU-8 (Microchem, SU-8 2075) mold was fabricated in another SOP. Liquid PDMS was poured onto the SU-8 mold, then covered by a silicon

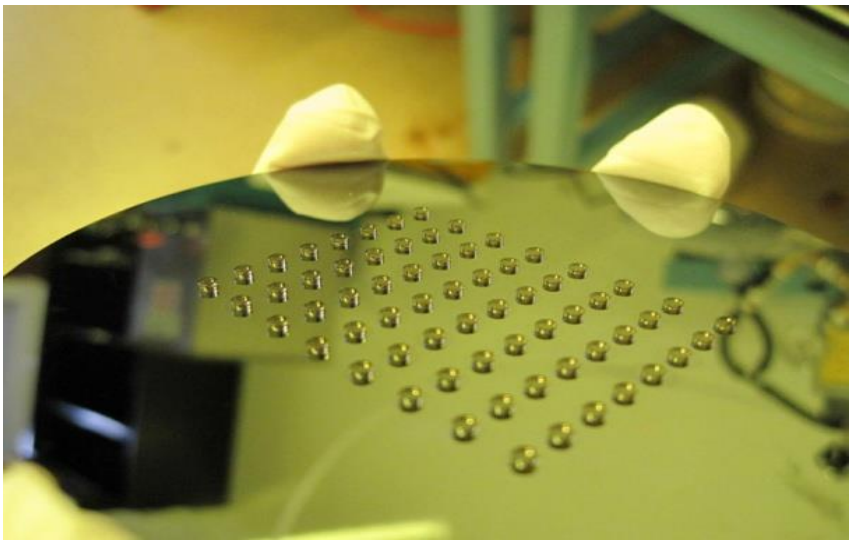

Fig. 2.14 The SU-8 2075 mold

wafer. After curing at 65℃ for 12 hours, the porous PDMS layer with pre-molded holes (2.5mm in diameter) was peeled off from the mold.

#2: Both sides of the pressure-sensitive rubber film (PCR Technical) were metalized by sputtering a layer of 30nm Au. Then, the film was punched to amass cylinder-shaped sensing elements 2mm in diameter.

#3: Laminate the e-skin. First, the electrode layers were trimmed to the sensor array's dimension (68 by 72 mm). Next, the surfaces of the electrode layers and porous layer were treated with oxygen plasma for adhesion (Pressure: 30torr, Power: 100 Watts, Time: 10s). Then the cylinder-shaped elements were placed into the holes in the middle layer. Finally, the middle layer is sandwiched between the two electrode layers to form an e-skin sensor as shown in Fig. 2.15. The upper and lower layer should be laid perpendicular with each other.

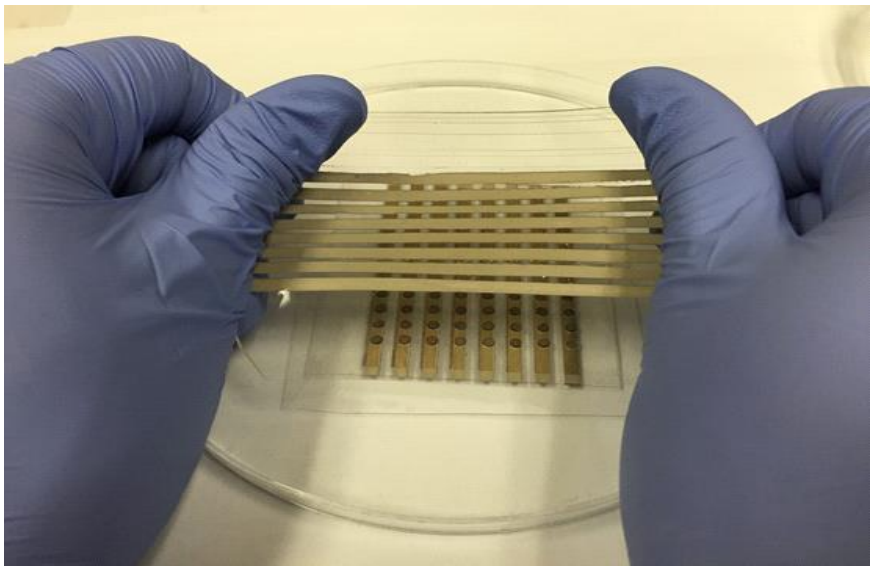

Fig. 2.15 Exploded view of the assembled e-skin sensor

CHAPTER 3

Performance Testing of Sensor System the Under Bending Deformation and Applied Force

After working out the best routine to fabricate the high flexible electrodes and setup the data collection system, we come to the most exciting part: sensor test. Currently no efforts have been made to investigate the mechanical behaviors of the tubular-shaped e-skin when bent, which is the typical working condition for the sensor when wrapping around the colonoscope. Here, in order to improve the sensor's reliability and accuracy, we conducted both mathematical simulation and experimental studies on the change in pressure distribution of our tubular shaped sensor under various bending conditions, with and without external pressure. In addition, the internal pressure of the tubular-shaped sensor, which is generated by deformation of the tube, has been figured out. Based on this, the actual relationship between sensor output and measured pressure will be obtained.

3.1 The Pressure-Resistance Characterization of Sensor Cell

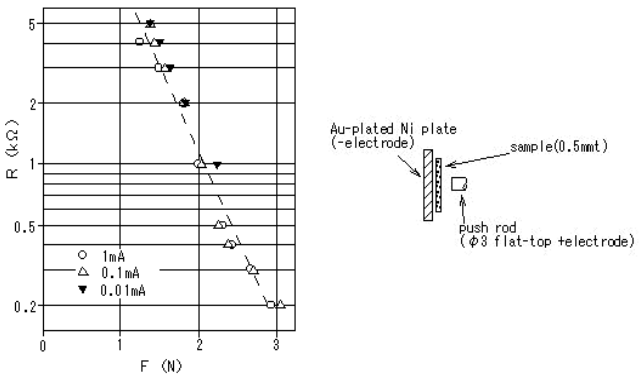

Fig. 3.1 Property of the piezo-resistive rubber provided by manufacuture(PCR Japan)

As the sensor is assembled, the sensing property of the piezo-resistive sensor cells is needed to be figured out. Figure 3.1 shows the manufacture's reference data sheet. Since contact resistance may exist between sensor cells and conducting strips, a load

Fig. 3.2 Experimental set-up for piezoresistive characterization of the sensor cells

cell and high resolution multi-meter was used to provide constant vertical force and display resistance value which works as an accurate reference for our further test.

The sensor patch is placed on the planer substrate of a weigh scale, the load cell was held by an Epson Scara G3 robot, a voltage division circuit and a Phidget Interface Kit 8/8/8 is designed to measure the resistance of the sensing elements. With the increase of the pressure, the resistance change of the sensor cells was observed and the value of the resistance was recorded by the computer. The obtained relation between the resistance and the applied pressure on sensor cells is show in Fig.3.3. Each data point in the figure was obtained by averaging 10 measurements on one sample at a specific applied pressure.

3.2 Internal Pressure Investigation

To examine the intrinsic pressure generated by deformation of the tube(colonoscope), a bending test was conducted for our tubular shaped sensor, Eight plastic pipes with different radii (55mm, 70mm, 100mm, 150mm, 200 mm, 280mm, 350mm and 450mm) were prepared for the bending tests. The prototype was bent against each pipe's outer circumference in order to generate 8 different bending

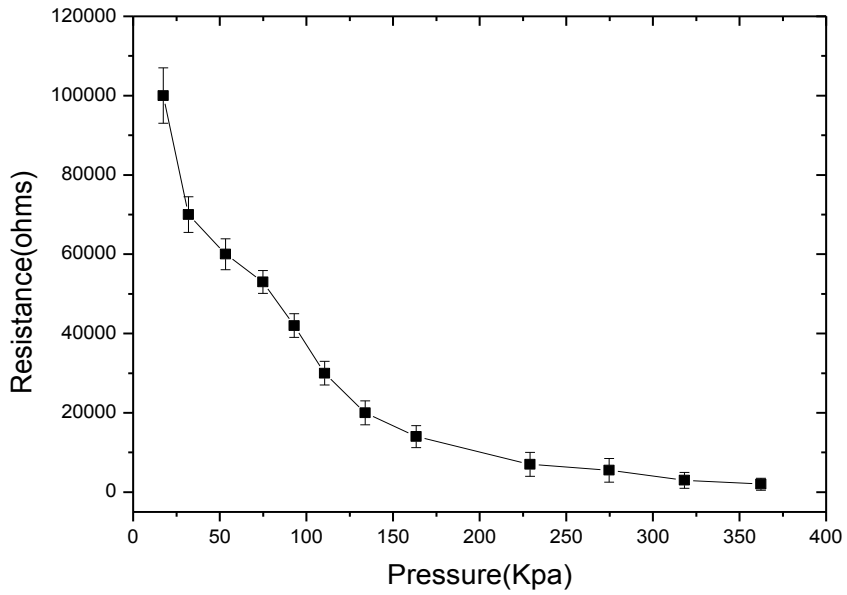

Fig. 3.3 Piezo-resistive response of sensor with pressure

curvatures. For each test, the colonoscope was bent-released 5 times with different orientation to ensure the measurement accuracy.

Figure. 3.3 shows the data acquisition system used for signal collection in the experiment. It includes a Phidget Interface Kit 8/8/8 which used as a data acquisition device, the e-skin sensor and a computer for data collection and processing. By wrapping the colonoscope with our e-skin sensor to the cylinder with different

curvatures, the relationship between the measured pressure and the bending curvature was obtained and is shown below. Our study focused on the elements that were aligned on the outermost perimeter of a bent colonoscope since these elements are at the locations with the largest bending curvature and sustain the most deformation, and therefor suffer the greatest pressure during a colonoscopy.

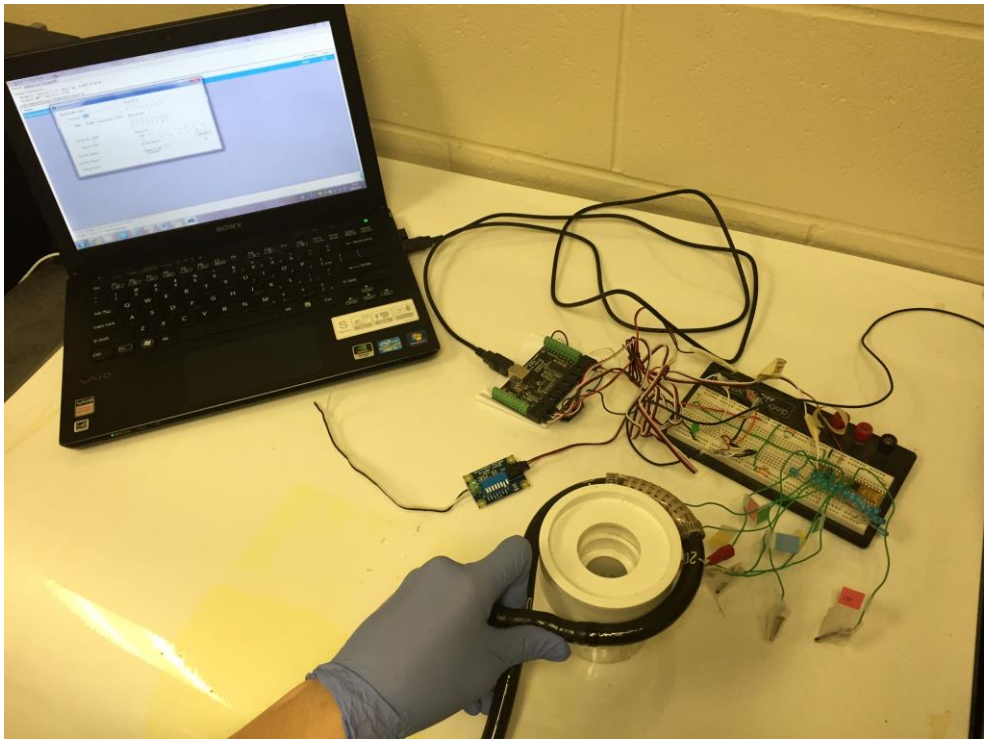

Fig. 3.4 Bending test of the tactile-sensor system(without applied pressure)

From Fig.3.5, it is observed that the bending deformation may lead to an internal pressure of 34~38 kPa in the e-skin sensor when the bending curvature of the colonoscope changes from 450mm to 50mm. It is also observed that smaller bending radius generates higher pressure due to larger bending deformation. Under significant deformation (radius < 100mm), the sensor elements sustained a relatively high pressure; as the deformation reduced (radius > 100mm), the deformation pressure may drop and the value will be around 34kPa at 450mm radius.

As long as the pressure due to bending deformation at different curvatures could be compensated during colonoscopy, the accurate measurement of the pressure due to the contact between colon wall and colonoscope can be achieved. However, we can only investigate limited number of curvatures. To further investigate the pressure due to bending at any curvature, a mathematic model was built to simulate the sensor's deformation during bending.

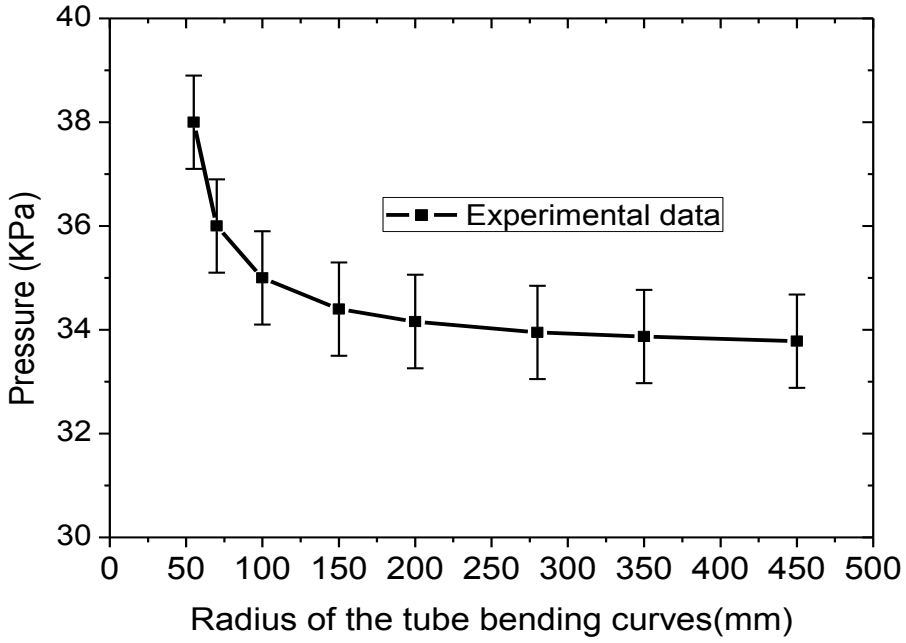

Fig. 3.5 Experimental results: bending curvature vs internal pressure

3.3 Mathematical Modeling and Simulation

Since testing can only provide data on certain curvatures, a mathematical model could compensate for unwanted pressure (systematic error) at any curvature. To reach this goal, a three dimensional mathematical model was built based on Hertzian non-adhesive elastic theory [57]. The contact between the surface of the PDMS layer and the upper/lower surface of a circular piezo-resistive element is non-conforming.

Moreover, these two materials are dissimilar enough to describe the contact area as a small ellipse as required by the classic standard definition.

The deflections and subsurface stresses resulting from the contact pressure are then evaluated with the following assumptions [63]: (1) the material is homogeneous; (2) the contact is over a small area relative to the material size; (3) the radii of the curvature of the contacting surfaces are substantially greater than the radius of the contact surface; and (4) the surfaces are frictionless. In our e-skin sensor array, the PDMS layer is homogenous after spinning coating, degassing and curing, the sensing elements are made from a type of flexible silicon rubber based composite. Both the PDMS layer and sensing layer have consistent physical properties and stable mechanical behaviors. The requirement for frictionless surface indicates that only a normal compressive stress exists over the contact surface and that there is no tangential force. In this work, the contact pressure simply leads to a uniaxial loading between the small cylinder of the sensing element and the PDMS substrate. So the internal deformation in the sensor array is invariant with the elastic deformation, which appeals to the assumptions of the Hertz contact theory.

The maximum contact pressure brought by the contact force *Q* in Newton (N) at the center of the contact surface, known as σ_{max} in Pa, is given by Kikuchi [64]:

$$\sigma_{max} = \frac{3}{2}\left[\frac{Q}{\pi ab}\right], \qquad (1)$$

where *a* and *b* are major and minor axes of the contact area and they can be obtained using (2) and (3),

$$a = m\left[\frac{3Q}{2E_c\sum\rho}\right]^{1/3}, \qquad (2)$$

$$b = n\left[\frac{3Q}{2E_c\sum\rho}\right]^{1/3}, \qquad (3)$$

E_c and $\sum\rho$ can be expressed as:

$$\frac{1}{E_c} = \frac{1-v_1^2}{E_1} + \frac{1-v_2^2}{E_2}, \qquad (4)$$

$$\sum\rho = \rho_1 + \rho_1^{'} + \rho_2 + \rho_2^{'}, \qquad (5)$$

where, E is the Young's modulus in Pascal of the contact body, v is Poisson's ratio, and subscripts 1 and 2 refer to two bodies, i.e., "1" is for the sensing element and "2" is for the PDMS substrate, r_i and $r_i^{'}$ define the minimum and maximum radii of curvature. In this problem, they could be transferred from the radius of tubular e-skin and the radius of sensing element, respectively.

The combined deformation d of two bodies along the axis of load can be expressed as:

$$\delta = \frac{k}{2}\left(\frac{9Q^2}{\pi^2 E_c^2}\sum\rho\right)^{1/3}, \qquad (6)$$

where k is a dimensionless factor drawn upon the principal curvature of the bodies, m and n both can be expressed and solved by k [65].

Complete elliptic integral is used as intermediate variables in the mathematic model. The complete elliptic integral of the first kind U and the second kind V are defined as

$$U = \int_0^{\pi/2} \frac{1}{\sqrt{1-k^2 \sin\varphi^2}} d\varphi, \tag{7}$$

$$V = \int_0^{\pi/2} \sqrt{1-k^2 \sin\varphi^2}\, d\varphi, \tag{8}$$

Based on Eqs.(7) and (8), the relationship between k and the curvature coefficients m, n as long as the curvature difference Y could be expressed using U and V.

$$m = \left(\frac{1}{1-k^2} \frac{2V}{\pi} \right)^{1/3}, \tag{9}$$

$$n = \left(\sqrt{1-k^2} \frac{2V}{\pi} \right)^{1/3}, \tag{10}$$

$$Y = \frac{\left|\rho_1 - \rho_1'\right| + \left|\rho_2 - \rho_2'\right|}{\sum \rho} = \frac{(2-k^2)V - 2(1-k^2)U}{k^2 V}, \tag{11}$$

where different values of k expresses different conditions. Under certain contact, with the definite principle curvature, k is constant.

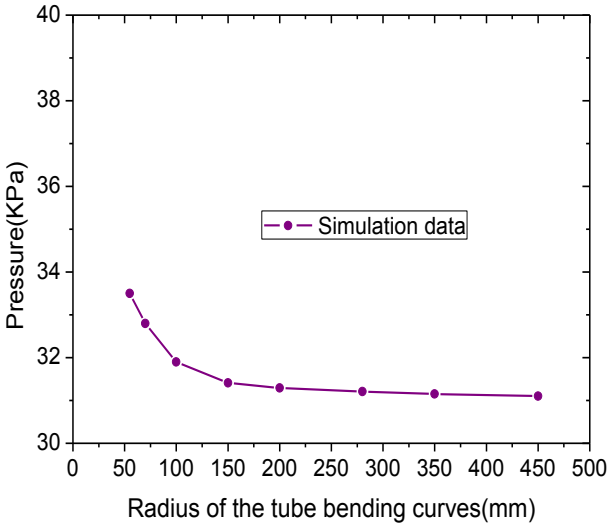

Fig. 3.6 Simulation results: bending curvature vs internal pressure

In the simulation, the following values are used: For the piezoresistive sensing

element, E_1 = 0.86MPa, v_1 = 0.490, and the radius of each sensing element is 1mm; For the PDMS substrate layer E_2 = 1.80Mpa, v_2 = 0.4999, the radius of the e-skin tube is 6.56mm. By plugging these geometrical and mechanical parameters into the above formulas, the critical contact pressure can then be calculated and the simulation results were summarized in Fig. 5.6. The internal pressure drops from 33.5 kPa to 31.2 kPa when the radius of the innermost curve of the colonoscope changes from 50mm to 450mm. In addition, it will continue to drop to 0 when the bend radius approaches infinity, in which case no deformation happens.

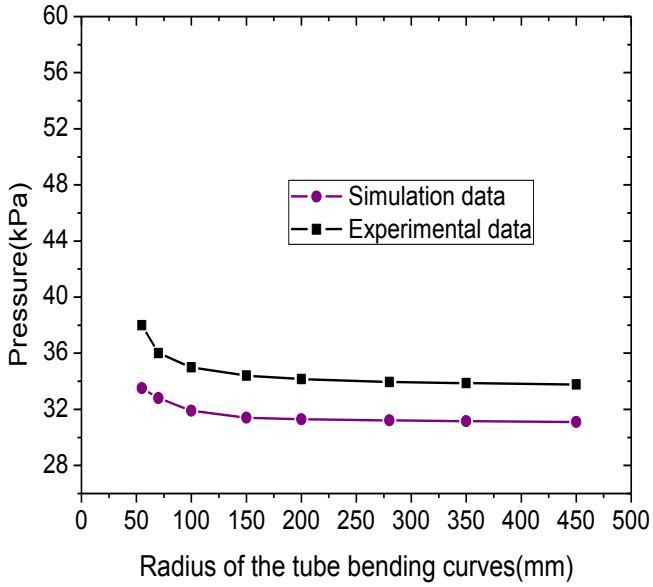

Fig. 3.7 Comparison between experimental and simulation results

From the results, it is observed that this e-skin is capable of detecting contact pressure under various practical conditions. Fig.3.5 demonstrated that in bending experiments, as the extent of the deformation becomes smaller, the internal pressure will reduce from 38kpa to 33.8kpa. The simulation results suggested a good agreement with the experimental data based on the results in Fig.3.6. The

experimental and simulation results demonstrated the same variation trend and similar amplitude as Fig3.7 shows, which exhibits the reliability of our sensor array. However, by comparing the experimental and simulation results, we observed a difference of 8%. It is noted, we need to recognize the contact resistance between the contact surfaces of the sensing element and the AgNWs conductive strip as a considerable factor.

3.4 Sensor Test with Applied Force

Once methods of obtaining systematic error caused by pressure on the sensory cells during bending were obtained, the data as reference was tested against pressure readings caused by external load on the sensory layer while under bending deformation. This was done to ascertain the percentage accuracy of both the experimental error curve, and the mathematical model in order to validate the

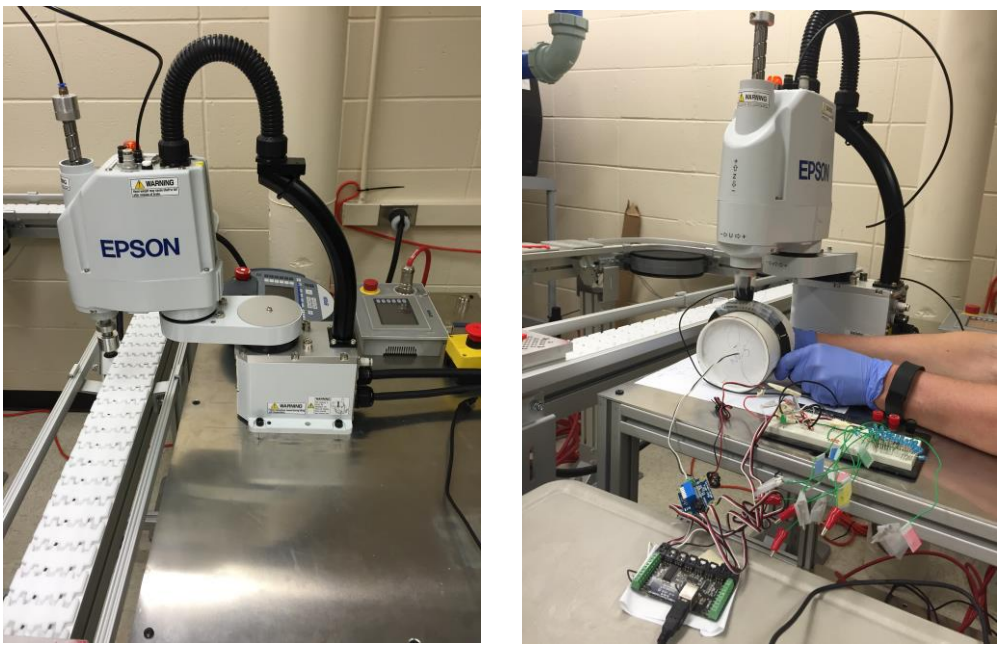

Fig. 3.8 Recalibrate the robot and conduct experiment taken with constant external pressure applied by Epson Scara G3 robot

decrease in error under bending when either method was applied to the final pressure reading of the sensory layer.

The tactile sensor was wrapped around a colonoscope with various radii, while hooked up to a data acquisition circuit. This is to obtain a final reading from the sensor once an external load was applied. The data acquired was then to be compared with previously obtained pressure reading which were limited to internal pressure caused by bending.

The Epson Scara G3 was used to assist in the application of pressure onto the tactile sensor layer while under bending deformation as seen in Fig. 3.8. The Scara G3 was able to provide and maintain accurate and even pressure on the sensory layer, so as to reduce any human error during the test. The #5 radius pipe was selected, as it's the median within the previously used range of radiuses.

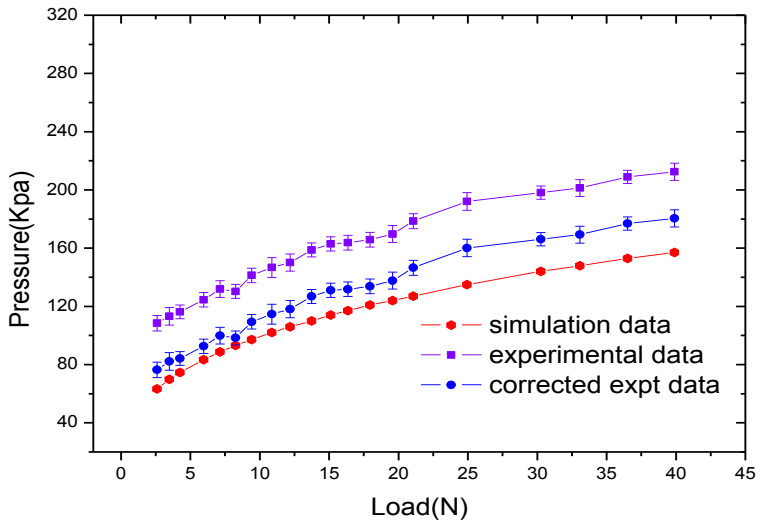

Fig. 3.9 Comparison of corrected experimental data with simulation data when bent against 200mm radii pipe

After testing was done by applying external load to the sensor layer and

recording the uncorrected pressures, these readings were then corrected against error due to bending, and this was compared to the simulated corrected pressure (Fig.3.9). The uncorrected pressure reading had an average variance of 35% from the calculated pressure, and after correcting for error, the average variance was 9%. This demonstrates the importance of correcting for internal pressure due to bending, as well as validating the increase in accuracy based on the application of the curves generates to calculate error based on the bending radius.

CHAPTER 4

Pressure Detection in Colon-Simulator

With the thorough investigation about the tactile sensor, the resistance-pressure relation is obtained, and internal pressure of various bending curvature is clarified, accurate applied pressure measurement is successfully achieved. Based on these, our ultimate goal of conducting real time pressure detection inside colon wall will be approached. In this section, two sensor patches were integrated on a PVC hose(similar size with colonoscope) in series, both of them are connected with the D/A system, when external pressure applied on the tube, the location and intensity will be directly converted into the brightness of pixels on GUI and shown simultaneously.

4.1 Colon Simulator

As we discussed in Chapter 1, colonoscopy is a test with certain rate of fatal threats which can hardly be rid off by cautious manipulation. In addition, the human colon constantly change its orientation in the abdomen, which makes colonoscopy a particularly experience demanding medical procedure. The "Colonoscope Simulation

Fig. 4.1 Colonoscope training mode by Kyoto Kagaka.Co

Training Model" developed by Kyoto Kagaku Co. is primarily used for the training of medical professionals, it has the same life-size with adults, which is a perfect prototype for our initial integration with the sensor system we built.

The colon simulator composed of abdomen model, colon-rectum tube, anus unit, skin cover and fixture set. The soft, flexible and airtight material allows realistic colonoscope insertion training, and the lids of both ends can be taken off so that we can educe the signal out. In addition, this training body may be oriented in either the left lateral, right lateral or supine position. Moreover, five different layout guides with six cases can be adjusted as well. Multiple examination mode are available for our examination.

4.2 Insertion Test and Real Time Pressure Detection

To better serve our goal of full scale pressure detection for the long, thin colonoscope,

Fig. 4.2 Two sensor patches integrated on the tube

we downsize the sensor patch to a 4*6 array and connect two of them in series for larger area coverage on the tube. By similar approach described in the previous chapter, two dragon skin based sensor patches are fabricated with whole thickness of 0.6mm. Carbon based conductive glue is applied to stick wires(0.025mm,silver-coated copper wires) onto the end of each conducting AgNW strips on the sensor, then the whole structure is wrap around a PVC braided hose with diameter of 1.2mm.

The whole tube was inserted into the colon-simulator through the bottom, with

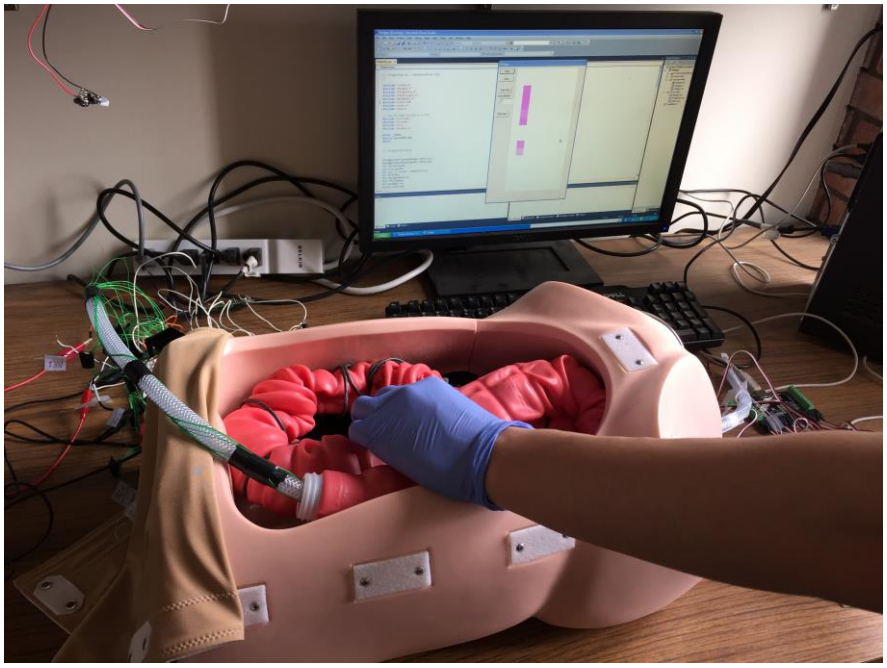

Fig. 4.3 Real time pressure detection in colon-simulator when apply pressure on sensor

all the wires around the tube connected to the scanning power supply circuit and the eight wires along axial direction linked with the eight channel data acquisition system. By using the scanning power supply circuit (as we discussed in chapter 2), at one moment, only one row is powered with 5V voltage, and each one of the column along the axial direction is corresponding to one data reception channel, thus the pressure on

every pixel can be measured. In addition, since all the resistance changes that generated by applied pressure will be converted into brightness value variation and displayed on the computer, the real-time visualized pressure detection is achieved

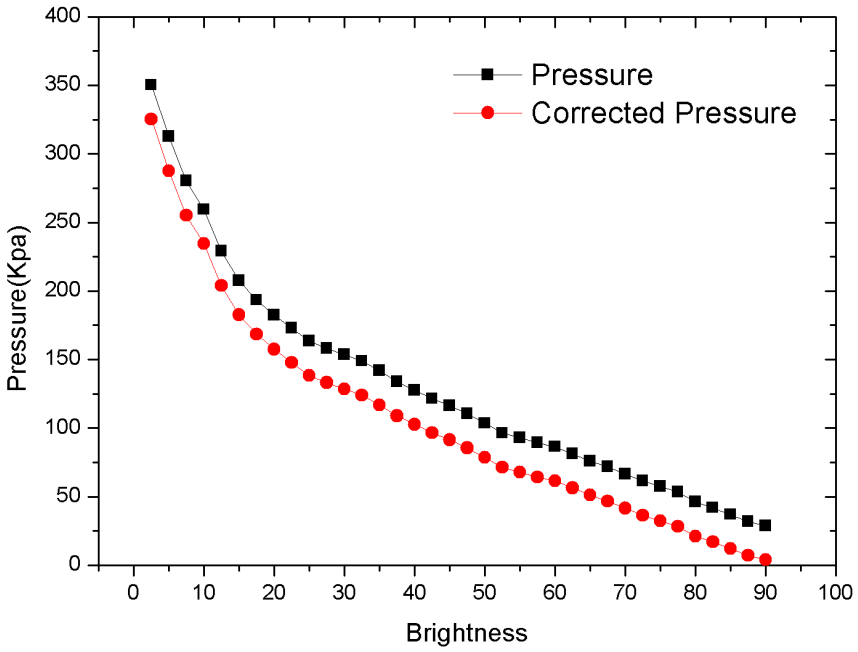

Fig. 4.4 Relationship between brightness value and applied pressure with bending curvature of

here. Furthermore, as the scanning frequency is adjustable up to 1KHz, it's easy to get the whole pressure distribution of the entire coverage area within milliseconds.

As the figure demonstrates above, unconstant pressure is applied on one sensor cell by hand, under high scanning frequency, the increase, release and unloading of external force can be displayed on screen directly. The change of square brightness is correlated to the fluctuation of brightness value, which is caused by the resistance change generated by external force applied. A relationship between brightness and pressure is obtained and shown in Fig. 3.4. By compensating the systematic error, we can identify when the square looks totally dark, the correspondent pressure is around

325 Kpa which is also the test limit of current system. When no external pressure is applied, the square will not show wholly blank with brightness of 90. Meanwhile, since there is no brightness change on any other rows on the GUI, we can tell that no crosstalk among our sensor system.

CHAPTER 5

Conclusion and Future Recommendations

To sum up, in this research work, a new type of highly flexible and stretchable tubular shaped tactile sensor array is designed and fabricated based on highly compliant silicone base, piezo-resistive rubber and silver nanowire. Ultra-thin, high conductivity and long-term reliable electrode layers are obtained and four different metallization routines are investigated. The e-skin sensor was able to withstand significant large deformation. Then, the contact pressures between sensing elements and the electrode substrate layers were experimentally investigated under the conditions of with and without the presence of external compressive force. The experimental results proved the capability of the sensor array to detect deformation pressure under various bending statuses. In addition, a mathematical model based on Hertzian contact theory was built to obtain numerical evaluation of the contact pressure. The deformation pressure caused by bending is identified and compensated successfully in following the test. Finally, real-time pressure detection inside colon simulator is performed and a visualized and accurate pressure distribution is obtained. Pressure dictation with less systematic error and higher accuracy can be achieved during a colonoscopy. This research work could provide an important technic for upgrading the strategies of colonoscopy for higher safety tests, and help make it a more predictable and less physical threat examination.

The prospect of automating the procedure for fabricating our high flexible e-skin

comes from the aim to get uniform and large area products with short time and low cost. By reviewing the state-of-art technics of large-scale automated production, it is noted that tradeoffs like less-spatial resolution, loss of conformability and non-responsiveness did happen since the problems about how to integrate those novel nanomaterials nicely with available fabrication instruments are still not addressed [12, 13, 66, 67]. In brief, regulating the random network of carbon nanotubes or metal-nanowires is a tricky task based on a traditional routine. In our three layer sensor, AgNWs which are used as conducting electrode, exist as a kind of suspension state in ethanol solvent with concentration of 10mg/ml. In fact, the suspension of AgNWs can only be stable for 7 weeks in room temperature, after this period of time, NWs gradually stick to each other and form irreversible clumps, the conductance will drop accordingly[49]. In order to assure sensor with consistent property can be obtained, we plan to get our solution processed AgNWs first, then setup Meyer rod to reduce the bundle and re-decomposed in PVP, at last we can use slot extrusion die or nozzle tip to inject the solution processed AgNWs into silicone matrix at certain depth by 3D printer. The detailed steps should be:

1. Certain volume of nanowire suspension is dropped on a glass substrate with 100-nm-thick prepatterned Ag contact pads and is allowed to dry in air for 10 min while agitated on a shaker or in a centrifuge.

2. The resulting films should be random meshes of AgNWs without significant bundling of wires that are spread over the area of the substrate, annealing of the meshes at a temperature of370~400 F.

3. A Meyer rod is either pulled or rolled over the solution, leaving a uniform, thin layer of Ag NW mesh.

4. Re-decompose this thin layer of mesh in PVP(poly-vinyl pyrrolidone) to allow the NWs make contact and fuse with each other instead of stick as a cluster.

5. The newly-processed AgNW solution will work perfectly as a raw material for a nozzle tip to inject into all type of flexible polymers in certain depth by 3-D printer.

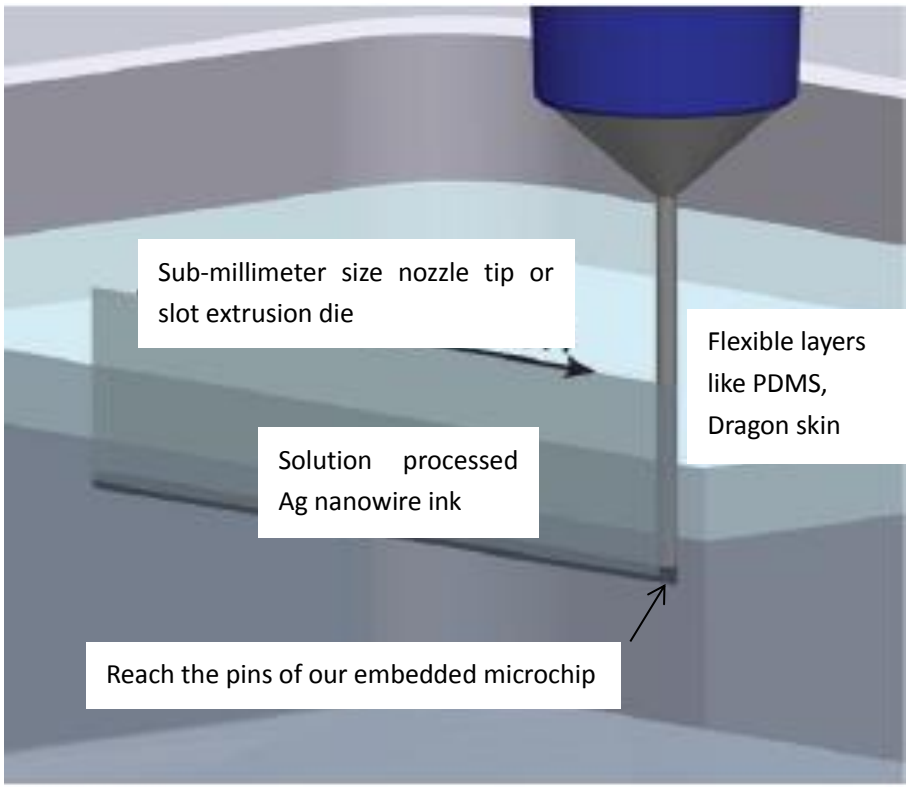

Fig. 5.1 Illustration of the 3-D injection process by 3D-printer and suitable nozzle tip

Since we can get mi**c**rochip by AMI0.5 technology, the microchip which work as signal transmission is down sized to sub-millimeter range, with can be easily embedded within our flexible sensor layer and keep unaffected by any type of bending. Thus, by injecting the processed AgNWs to connected the pins of microchip, our tactile sensor can be turned into an ultra-light and thin, high responsive and

flexible, long-term stable e-skin for literally any type of curved surface in medical instrument and health care robots.

References

[1] T. Uraoka, N. Hosoe, and N. Yahagi, "Colonoscopy: is it as effective as an advanced diagnostic tool for colorectal cancer screening?," *Expert Review of Gastroenterology & Hepatology,* vol. 9, pp. 129-132, Feb 2015.

[2] G. Arora, A. Mannalithara, G. Singh, L. B. Gerson, and G. Triadafilopoulos, "Risk of perforation from a colonoscopy in adults: a large population-based study," *Gastrointestinal Endoscopy,* vol. 69, pp. 654-664, Mar 2009.

[3] T. Xu, W. Wang, X. Bian, X. Wang, X. Wang, J. K. Luo, *et al.*, "High resolution skin-like sensor capable of sensing and visualizing various sensations and three dimensional shape," *Scientific Reports,* vol. 5, Aug 13 2015.

[4] J. A. Rogers, Z. Bao, K. Baldwin, A. Dodabalapur, B. Crone, V. R. Raju, *et al.*, "Paper-like electronic displays: Large-area rubber-stamped plastic sheets of electronics and microencapsulated electrophoretic inks," *Proceedings of the National Academy of Sciences of the United States of America,* vol. 98, pp. 4835-4840, Apr 2001.

[5] D. H. Kim, J. L. Xiao, J. Z. Song, Y. G. Huang, and J. A. Rogers, "Stretchable, Curvilinear Electronics Based on Inorganic Materials," *Advanced Materials,* vol. 22, pp. 2108-2124, May 2010.

[6] T. Sekitani and T. Someya, "Stretchable, Large-area Organic Electronics," *Advanced Materials,* vol. 22, pp. 2228-2246, May 2010.

[7] M. H. Lee, "Tactile sensing: New directions, new challenges," *International Journal of Robotics Research,* vol. 19, pp. 636-643, Jul 2000.

[8] P. Puangmali, K. Althoefer, L. D. Seneviratne, D. Murphy, and P. Dasgupta, "State-of-the-art in force and tactile sensing for minimally invasive surgery," *Ieee Sensors Journal,* vol. 8, pp. 371-381, Mar-Apr 2008.

[9] R. D. Howe, W. J. Peine, D. A. Kontarinis, and J. S. Son, "REMOTE PALPATION TECHNOLOGY," *Ieee Engineering in Medicine and Biology Magazine,* vol. 14, pp. 318-323, May-Jun 1995.

[10] S. Katsura, Y. Matsumoto, and K. Ohnishi, "Modeling of force sensing and validation of disturbance observer for force control," *Ieee Transactions on Industrial Electronics,* vol. 54, pp. 530-538, Feb 2007.

[11] S. Schostek, C. N. Ho, D. Kalanovic, and M. O. Schurr, "Artificial tactile sensing in minimally invasive surgery - a new technical approach," *Minimally Invasive Therapy & Allied Technologies,* vol. 15, pp. 296-304, Oct 2006.

[12] H. Yousef, M. Boukallel, and K. Althoefer, "Tactile sensing for dexterous in-hand manipulation in robotics-A review," *Sensors and Actuators a-Physical,* vol. 167, pp. 171-187, Jun 2011.

[13] M. I. Tiwana, S. J. Redmond, and N. H. Lovell, "A review of tactile sensing technologies with applications in biomedical engineering," *Sensors and Actuators a-Physical,* vol. 179, pp. 17-31, Jun 2012.

[14] S. Park, H. Kim, M. Vosgueritchian, S. Cheon, H. Kim, J. H. Koo, *et al.*, "Stretchable Energy-Harvesting Tactile Electronic Skin Capable of Differentiating Multiple Mechanical Stimuli Modes," *Advanced Materials,* vol. 26, pp. 7324-7332, Nov 2014.

[15] S. Aoi, Y. Egi, A. Ichikawa, and K. Tsuchiya, *Experimental Verification of Gait Transition from Quadrupedal to Bipedal Locomotion of an Oscillator-driven Biped Robot*. New York: Ieee, 2008.

[16] P. M. Grice, M. D. Killpack, A. Jain, S. Vaish, J. Hawke, and C. C. Kemp, "Whole-arm tactile sensing for beneficial and acceptable contact during robotic assistance," *IEEE ... International Conference on Rehabilitation Robotics : [proceedings]*, vol. 2013, pp. 6650464-6650464, 2013-Jun 2013.

[17] T. L. Chen, C. H. A. King, A. L. Thomaz, and C. C. Kemp, "An Investigation of Responses to Robot-Initiated Touch in a Nursing Context," *International Journal of Social Robotics,* vol. 6, pp. 141-161, Jan 2014.

[18] M. L. Hammock, A. Chortos, B. C. K. Tee, J. B. H. Tok, and Z. A. Bao, "25th Anniversary Article: The Evolution of Electronic Skin (E-Skin): A Brief History, Design Considerations, and Recent Progress," *Advanced Materials,* vol. 25, pp. 5997-6037, Nov 2013.

[19] N. Wettels, V. J. Santos, R. S. Johansson, and G. E. Loeb, "Biomimetic tactile sensor array," *Advanced Robotics,* vol. 22, pp. 829-849, 2008.

[20] L. H. Wang and Y. L. Li, "A Review for Conductive Polymer Piezoresistive Composites and a Development of a Compliant Pressure Transducer," *Ieee Transactions on Instrumentation and Measurement,* vol. 62, pp. 495-502, Feb 2013.

[21] J. B. H. Tok and Z. A. Bao, "Recent advances in flexible and stretchable electronics, sensors and power sources," *Science China-Chemistry,* vol. 55, pp. 718-725, May 2012.

[22] M. A. McEvoy and N. Correll, "Materials that couple sensing, actuation, computation, and communication," *Science,* vol. 347, p. 9, Mar 2015.

[23] J. Meyer, B. Arnrich, J. Schumm, and G. Troester, "Design and Modeling of a Textile Pressure Sensor for Sitting Posture Classification," *Ieee Sensors Journal,* vol. 10, pp. 1391-1398, Aug 2010.

[24] T. Someya, T. Sekitani, S. Iba, Y. Kato, H. Kawaguchi, and T. Sakurai, "A large-area, flexible pressure sensor matrix with organic field-effect transistors for artificial skin applications," *Proceedings of the National Academy of Sciences of the United States of America,* vol. 101, pp. 9966-9970, Jul 2004.

[25] Q. Cao, H. S. Kim, N. Pimparkar, J. P. Kulkarni, C. J. Wang, M. Shim, *et al.*, "Medium-scale carbon nanotube thin-film integrated circuits on flexible plastic substrates," *Nature,* vol. 454, pp. 495-U4, Jul 2008.

[26] K. Takei, T. Takahashi, J. C. Ho, H. Ko, A. G. Gillies, P. W. Leu, *et al.*, "Nanowire active-matrix circuitry for low-voltage macroscale artificial skin," *Nature Materials,* vol. 9, pp. 821-826, Oct 2010.

[27] C. Wang, D. Hwang, Z. B. Yu, K. Takei, J. Park, T. Chen, *et al.*, "User-interactive electronic skin for instantaneous pressure visualization,"

Nature Materials, vol. 12, pp. 899-904, Oct 2013.

[28] D. J. Lipomi, M. Vosgueritchian, B. C. K. Tee, S. L. Hellstrom, J. A. Lee, C. H. Fox, *et al.*, "Skin-like pressure and strain sensors based on transparent elastic films of carbon nanotubes," *Nature Nanotechnology,* vol. 6, pp. 788-792, Dec 2011.

[29] M. Ramuz, B. C. K. Tee, J. B. H. Tok, and Z. N. Bao, "Transparent, Optical, Pressure-Sensitive Artificial Skin for Large-Area Stretchable Electronics," *Advanced Materials,* vol. 24, pp. 3223-3227, Jun 2012.

[30] B. C. K. Tee, C. Wang, R. Allen, and Z. N. Bao, "An electrically and mechanically self-healing composite with pressure- and flexion-sensitive properties for electronic skin applications," *Nature Nanotechnology,* vol. 7, pp. 825-832, Dec 2012.

[31] M. Ying, A. P. Bonifas, N. S. Lu, Y. W. Su, R. Li, H. Y. Cheng, *et al.*, "Silicon nanomembranes for fingertip electronics," *Nanotechnology,* vol. 23, p. 7, Aug 2012.

[32] M. S. Mannoor, H. Tao, J. D. Clayton, A. Sengupta, D. L. Kaplan, R. R. Naik, *et al.*, "Graphene-based wireless bacteria detection on tooth enamel," *Nature Communications,* vol. 3, p. 8, Mar 2012.

[33] J. Park, Y. Lee, J. Hong, Y. Lee, M. Ha, Y. Jung, *et al.*, "Tactile-Direction-Sensitive and Stretchable Electronic Skins Based on Human-Skin-Inspired Interlocked Microstructures," *Acs Nano,* vol. 8, pp. 12020-12029, Dec 2014.

[34] D. P. J. Cotton, I. M. Graz, and S. P. Lacour, "A Multifunctional Capacitive Sensor for Stretchable Electronic Skins," *Ieee Sensors Journal,* vol. 9, pp. 2008-2009, Dec 2009.

[35] T. Araki, M. Nogi, K. Suganuma, M. Kogure, and O. Kirihara, "Printable and Stretchable Conductive Wirings Comprising Silver Flakes and Elastomers," *Ieee Electron Device Letters,* vol. 32, pp. 1424-1426, Oct 2011.

[36] Y. K. Ohmura, Yasuo; Nagakubo, Akihiko, "Conformable and scalable tactile sensor skin for curved surfaces," *2006 IEEE INTERNATIONAL CONFERENCE ON ROBOTICS AND AUTOMATION (ICRA), VOLS 1-10* pp. 1348-1353, 2006

[37] X. L. Wang, H. Hu, Y. D. Shen, X. C. Zhou, and Z. J. Zheng, "Stretchable Conductors with Ultrahigh Tensile Strain and Stable Metallic Conductance Enabled by Prestrained Polyelectrolyte Nanoplatforms," *Advanced Materials,* vol. 23, pp. 3090-+, Jul 2011.

[38] Alamusi, N. Hu, H. Fukunaga, S. Atobe, Y. L. Liu, and J. H. Li, "Piezoresistive Strain Sensors Made from Carbon Nanotubes Based Polymer Nanocomposites," *Sensors,* vol. 11, pp. 10691-10723, Nov 2011.

[39] K. S. Kim, Y. Zhao, H. Jang, S. Y. Lee, J. M. Kim, K. S. Kim, *et al.*, "Large-scale pattern growth of graphene films for stretchable transparent electrodes," *Nature,* vol. 457, pp. 706-710, Feb 2009.

[40] T. Someya, A. Dodabalapur, J. Huang, K. C. See, and H. E. Katz, "Chemical and Physical Sensing by Organic Field-Effect Transistors and Related

Devices," *Advanced Materials,* vol. 22, pp. 3799-3811, Sep 2010.

[41] J. C. Lotters, W. Olthuis, P. H. Veltink, and P. Bergveld, "Polydimethylsiloxane as an elastic material applied in a capacitive accelerometer," *Journal of Micromechanics and Microengineering,* vol. 6, pp. 52-54, Mar 1996.

[42] B. H. Jo, L. M. Van Lerberghe, K. M. Motsegood, and D. J. Beebe, "Three-dimensional micro-channel fabrication in polydimethylsiloxane (PDMS) elastomer," *Journal of Microelectromechanical Systems,* vol. 9, pp. 76-81, Mar 2000.

[43] K. J. Regehr, M. Domenech, J. T. Koepsel, K. C. Carver, S. J. Ellison-Zelski, W. L. Murphy, *et al.*, "Biological implications of polydimethylsiloxane-based microfluidic cell culture," *Lab on a Chip,* vol. 9, pp. 2132-2139, 2009.

[44] S. K. Sia and G. M. Whitesides, "Microfluidic devices fabricated in poly(dimethylsiloxane) for biological studies," *Electrophoresis,* vol. 24, pp. 3563-3576, Nov 2003.

[45] T. R. Kline, M. L. Tian, J. G. Wang, A. Sen, M. W. H. Chan, and T. E. Mallouk, "Template-grown metal nanowires," *Inorganic Chemistry,* vol. 45, pp. 7555-7565, Sep 2006.

[46] H. Y. Sun, X. H. Li, Y. Chen, W. Li, F. Li, B. T. Liu, *et al.*, "The control of the growth orientations of electrodeposited single-crystal nanowire arrays: a case study for hexagonal CdS," *Nanotechnology,* vol. 19, p. 8, Jun 2008.

[47] H. Z. Geng, K. K. Kim, K. P. So, Y. S. Lee, Y. Chang, and Y. H. Lee, "Effect of acid treatment on carbon nanotube-based flexible transparent conducting films," *Journal of the American Chemical Society,* vol. 129, pp. 7758-+, Jun 2007.

[48] L. B. Hu, H. S. Kim, J. Y. Lee, P. Peumans, and Y. Cui, "Scalable Coating and Properties of Transparent, Flexible, Silver Nanowire Electrodes," *Acs Nano,* vol. 4, pp. 2955-2963, May 2010.

[49] J. Y. Lee, S. T. Connor, Y. Cui, and P. Peumans, "Solution-processed metal nanowire mesh transparent electrodes," *Nano Letters,* vol. 8, pp. 689-692, Feb 2008.

[50] P. Lee, J. Lee, H. Lee, J. Yeo, S. Hong, K. H. Nam, *et al.*, "Highly Stretchable and Highly Conductive Metal Electrode by Very Long Metal Nanowire Percolation Network," *Advanced Materials,* vol. 24, pp. 3326-3332, Jul 2012.

[51] J. Y. Woo, K. K. Kim, J. Lee, J. T. Kim, and C. S. Han, "Highly conductive and stretchable Ag nanowire/carbon nanotube hybrid conductors," *Nanotechnology,* vol. 25, p. 7, Jul 2014.

[52] J. D. S. Najarian, and A. A. Mehrizi, " Artificial tactile sensing in biomedical engineering," *McGraw-Hill,* 2009.

[53] A. Wisitsoraat, V. Patthanasetakul, T. Lomas, and A. Tuantranont, "Low cost thin film based piezoresistive MEMS tactile sensor," *Sensors and Actuators a-Physical,* vol. 139, pp. 17-22, Sep 12 2007.

[54] G. Canavese, S. Stassi, M. Stralla, C. Bignardi, and C. F. Pirri, "Stretchable and conformable metal-polymer piezoresistive hybrid system," *Sensors and*

Actuators a-Physical, vol. 186, pp. 191-197, Oct 2012.

[55] L. H. Wang, T. H. Ding, and P. Wang, "Effects of conductive phase content on critical pressure of carbon black filled silicone rubber composite," *Sensors and Actuators a-Physical,* vol. 135, pp. 587-592, Apr 2007.

[56] M. Knite, V. Teteris, A. Kiploka, and J. Kaupuzs, "Polyisoprene-carbon black nanocomposites as tensile strain and pressure sensor materials," *Sensors and Actuators a-Physical,* vol. 110, pp. 142-149, Feb 2004.

[57] V. L. Pushparaj, L. J. Ci, S. Sreekala, A. Kumar, S. Kesapragada, D. Gall, *et al.*, "Effects of compressive strains on electrical conductivities of a macroscale carbon nanotube block," *Applied Physics Letters,* vol. 91, p. 3, Oct 2007.

[58] C. Min and D. M. Yu, "Simultaneously Improved Toughness and Dielectric Properties of Epoxy/Graphite Nanosheet Composites," *Polymer Engineering and Science,* vol. 50, pp. 1734-1742, Sep 2010.

[59] M. Shimojo, A. Namiki, M. Ishikawa, R. Makino, and K. Mabuchi, "A tactile sensor sheet using pressure conductive rubber with electrical-wires stitched method," *Ieee Sensors Journal,* vol. 4, pp. 589-596, Oct 2004.

[60] C. Wang, D. Hwang, Z. Yu, K. Takei, J. Park, T. Chen, *et al.*, "User-interactive electronic skin for instantaneous pressure visualization," *Nature Materials,* vol. 12, pp. 899-904, Oct 2013.

[61] H. Sharma, A. K. Shukla, and V. D. Vankar, "Effect of titanium interlayer on the microstructure and electron emission characteristics of multiwalled carbon nanotubes," *Journal of Applied Physics,* vol. 110, p. 11, Aug 2011.

[62] E. Vassallo, R. Caniello, A. Cremona, D. Dellasega, and E. Miorin, "Titanium interlayer to improve the adhesion of multilayer amorphous boron carbide coating on silicon substrate," *Applied Surface Science,* vol. 266, pp. 170-175, Feb 1 2013.

[63] R. K. Vishwakarma, U. S. Shivhare, and S. K. Nanda, "Predicting Guar Seed Splitting by Compression between Two Plates Using Hertz Theory of Contact Stresses," *Journal of Food Science,* vol. 77, pp. E231-E239, Sep 2012.

[64] N. Kikuchi and J. T. Oden, *Contact Problems in Elasticity: A Study of Variational Inequalities and Finite Element Methods*: Society for Industrial and Applied Mathematics, 1988.

[65] B. J. Hamrock, D. Dawson, and L. R. Center, *Numerical Evaluation of the Surface Deformation of Elastic Solids Subjected to a Hertzian Contact Stress*: National Aeronautics and Space Administration, 1974.

[66] J. J. Boland, "FLEXIBLE ELECTRONICS Within touch of artificial skin," *Nature Materials,* vol. 9, pp. 790-792, Oct 2010.

[67] S. C. B. Mannsfeld, B. C. K. Tee, R. M. Stoltenberg, C. Chen, S. Barman, B. V. O. Muir, *et al.*, "Highly sensitive flexible pressure sensors with microstructured rubber dielectric layers," *Nature Materials,* vol. 9, pp. 859-864, Oct 2010.

Appendix: Publication from This Work

1. “Modeling and Experimental Investigation of the Maximum Stresses due to Bending in a Tubular-shaped Artificial Skin Sensor”,Debao Zhou, **Yuhang Sun**, Jing Bai, Eliah Hauser, Shufang Wang, and Baoguo Han. ***IEEE Sensors Journal***, 16(6):1549-1556, March, 2016.
2. “Conformable Skin-Like Conductive Thin Films with AgNWs Strips for Flexible Electronic Devices”, **Yuhang Sun**, Debao Zhou, Jing Bai, Eliah Hauser, Shufang Wang, Baoguo Han, Zhaomiao Liu. ***Sensors and Transducers Journal*** (ISSN: 2306-8515, e-ISSN 1726-5479), 191(8):72-77, August 2015.
3. "Design and Evaluation of a Highly Stretchable and Conductive Skin-Like Electrode for Tactile Sensors", **Yuhang Sun**, Debao Zhou, Jing Bai, Haopeng Wang and Jianguo Cao. ***18th Annual Nanotech Conference and Expo***, June 14-17, 2015, Washington DC, USA.